Final Report on Research in Experimental High Energy Physics

The Regents of the University of Minnesota

Sponsored Projects Administration,
Suite 450 McNamara Alumni Center,
200 Oak Street SE,
Minneapolis, MN 55455-2070

Report Number: DOE-Minnesota-ER40823.

Project period dates: 01/01/1994 04/30/2014

Lead PI ..... Roger W. Rusack

Administrative Contact: ..... Pat Jondahl, 612-626-2244, jonda001@umn.edu.

DOE/Office of Science Program Office: ..... High Energy Physics.

DOE/Office of Science Program Office Technical Contact: SC.HEPFOA@science.doe.gov

DOE Grant Number: ..... DE-FG02-94ER40823.

Research Areas

Experimental Research at the Energy, Intensity and Cosmic Frontiers.

January 6, 2016

Research Areas and Thrust Organization

Research Areas

Energy Frontier: ..... Roger Rusack.
Cosmic Frontier: ..... Priscilla Cushman.
Intensity Frontier: ..... Marvin Marshak.

Research Thrusts

CMS: ..... Roger Rusack
CDMS: ..... Priscilla Cushman
BESIII: ..... Ronald Poling.

Contents

1 Introduction and Executive Summary

This document provides a report of the research carried out by the experimental high energy physics groups of the University of Minnesota. Our program is broad and highly productive, and directly aligned with projects central to the DOE long-term strategy for High Energy Physics in the US. The DOE currently supports the experimental HEP research of ten members of the faculty of the University of Minnesota School of Physics and Astronomy. The areas of focus of the experimental group are hadron collisions at the highest energies with CMS, neutrino physics with MINOS, NOνA and LBNE, the direct detection of dark matter with CDMS, and charm physics with BESIII. This report covers the activities of the experimental groups.

In the past three years the groups supported by the DOE have all made significant progress and posted major successes. The Minnesota CMS group has played leading roles in five data analyses and has had major roles in detector operations, the data management and the detector upgrades that are planned for for the LHC and those that are planned for the high-luminosity LHC. The CDMS-II experiment held the lead in WIMP sensitivity over the last decade, and is still the most sensitive detector in the world in the low WIMP mass region, with a recent 3σ hint of 8 GeV/c^2 WIMP candidates in the silicon data. SuperCDMS, with three orders of magnitude better electron recoil background rejection, has been collecting data since October 2011. Since all dark matter experiments require a better understanding of neutron backgrounds to make further advances in sensitivity, Cushman has expanded the Minnesota effort on backgrounds to the national level, where she is leading a coordinated effort in neutron simulations for underground physics. The work of Mandic on 100 mm detectors both for Super-CDMS and beyond has advanced rapidly.

Also at the Intensity Frontier, the BESIII experiment has had a successful year of operation largely focused on searches for and studies of new "charmonium-like" states above $D\bar{D}$ threshold. At least one new state was observed, and there are hints of others. An intensive effort to understand their nature and gain new insight into the strong interaction continues. BESIII has also produced a large number of other results in charmonium decay and light-hadronic physics.

The University of Minnesota group has constructed the NOνA Ash River Far Laboratory in Northern Minnesota and is assembling and installing the NOνA far detector there. NOνA, together with T2K, offers the best prospect for progress on the questions of neutrino mass hierarchy and leptonic CP violation in the next decade, with NOνA likely to produce exciting physics results within the period of this proposal. Concurrently, the Minnesota Group has continued to operate the MINOS Far Detector and has worked cooperatively with other MINOS collaborators to publish a final analysis of MINOS data (including the world's most accurate determination of Δm^2_{23}) and transition MINOS to the new higher neutrino energy experiment MINOS+. Minnesota has also provided leadership to the LBNE Experiment, with major participation in the LBNE reconfiguration process and the ongoing quest to place the LBNE far detector deep underground.

Research into the physics of neutrinos was part of this grant until 2008, and since then it has been funded under a separate arrangement. The report that describes the neutrino research will be included in the final report of the DOE Cooperative Agreement DE-FC02-07ER41471.

In the academic year 2012 - 2013, we supported 21 graduate students with TAs and RAs and 10 Research Associates. Our ten-year average for PhD production is 3.1 experimental PhDs per year and 1.5 per year in theory. During the academic year we run three weekly seminars on theoretical physics, experimental high energy physics, and a joint lunch seminar with the cosmology group (which includes the Minnesota Institute for Astrophysics). Our excellent undergraduates are an

important part of our mission and have contributed substantially to our research. The majority are supported by University fellowships (UROP), research scholarships, summer programs (REU) and project funds. Departmental research support was also provided for new graduate students in their first two summers.

2 Physics at the Energy Frontier: CMS at the LHC

This document provides a report of the activities of the experimental high energy group of the University of Minnesota who are working at the Energy Frontier.

The discovery of a scalar boson at the LHC [1] has been the most-important discovery in particle physics since the observation of the W and Z bosons 30 years ago established the Standard Model model. Within the Standard Model, only one scalar particle is predicted: the Higgs boson. The scalar field of the Higgs is a new and unique class of physics – unlike all the known force carrier, the Higgs is not a gauge field and its ultraviolet corrections are sensitive to many types of new particles and phenomena. The next step for research into the nature of the new scalar is a detailed study of its couplings and a completion of precision measurements to confirm or to find flaws in the simple Standard Model structure of the scalar sector.

Another of the important discoveries of the last 30 years is the observation of neutrino mass, a mass which is not explained by the Standard Model. The very small value of the neutrino mass, compared to the mass of all other known massive particles, and the nature of its mass-term within the Lagrangian are both issues of great interest which may be addressed by restoring left-right symmetry to the Standard Model and providing a mass to the neutrino through a see-saw mechanism.

The third major question that motivates our research interest is the nature of dark matter. The existence of particle dark matter is strongly suggested by measurements from the Cosmic Frontier. The exact nature of the dark matter, however, remains mysterious despite both direct searches (such as CDMS) and searches at colliders. The Minnesota group has focused on the possibility that dark matter could be within the range of the LHC but eludes the efforts of the supersymmetry analysis groups.

The physics questions of the Higgs, neutrino mass, and dark matter provide the framework for our research at the highest energy machine. As experimentalists, we consider it important to both invent, develop and deploy excellent instrumentation, and to carry out leading analyses of the data produced by the instrumentation. In the original construction of CMS, the group has made extensive contributions to the construction and commissioning of both the electromagnetic and hadronic calorimeters. Members of the group have and continue to hold various management responsibilities for the organization of the experiment. We have completed and are actively pursuing a number of data analysis efforts, described in more detail below. We are leading in the development and construction of the upgrades to the CMS detector required to answer our leading physics questions.

In the following sections, we begin by discussing the group's overall contributions to specific formal positions that were held in CMS by group members. We then discuss the physics analyses that we have pursued during the grant period, and specific developments in detector calibration and physics object reconstruction. We then describe the the current activities on the upgrades.

2.1 Group Contributions and Organization

Our group consists of three faculty members, three postdocs and, currently, nine graduate students. The senior members of the group have held and continue to hold important leadership roles within the collaboration. Rusack, who was the electromagnetic calorimeter (ECAL) project manager for the calendar years 2009 and 2010, is now serving as one of the two conveners of the forward detector upgrade working group (FDUWG) for the HL-LHC. Mans continues to serve as the deputy international project manager for the hadron calorimeter (HCAL) and is also leading the US-CMS

HCAL Upgrade as a Level-2 manager, successfully passing the CD1 review of the project in August 2013. In the last year, Kubota has been named the Level-3 manager (both US and CMS) for the HCAL off-detector electronics in the upgrade.

Senior Research Associate Giovanni Franzoni, who left the group for a CERN staff position, has been a convener of the CMS Physics Data and Monte Carlo Validation (PDMV) team since the summer of 2012. The responsibility of this group is to ensure that the data analysis and the Monte Carlo productions are accurate, and recently has included the validation of new Monte Carlo tools for the upgrade.. This role required Franzoni to work on nearly every aspect of the production of physics results

Research Associate Dahmes spent approximately half of his time between 2009 to 2012 at CERN to lead a team responsible for deploying and maintaining the High Level Trigger menus used by CMS to collect collision data. At the same time he led our program to search for a heavy right-handed W bosons and right-handed neutrinos and has continued since the end of data taking in 2012. He also currently convenes a group which performs physics studies based on non-SUSY exotic signatures in the HL-LHC era. For the past three summers he has also given a series of lectures at the CERN summer school discussing the importance of triggering for LHC experiments.

Research Associate Kao joined our group in 2011 and has been based in Minnesota, dividing his time between hardware and data analysis projects which are described in more detail below.

We have recently hired Nicole Ruckstuhl as a Research Associate. Her PhD on the ATLAS experiment was "Searches for New Signatures in $\mu^{\pm}\mu^{\pm}$ events." She will be stationed at CERN working on the installation and operation of the new hardware for the HCAL upgrade and data analysis.

Research associate Rekovic, who devoted all of his efforts during the last grant period to the Higgs $\rightarrow \gamma\gamma$ analysis has left the group in 2011 to join the CMS group at Rutgers.

In the past three years we have graduated four PhD students: Jason Haupt, Seth Cooper, Phil Dudero, and Abraham DeBenedetti. Kevin Klapoetke is the last of our first-generation CMS students. We are currently partially supporting with DOE funds six graduate students and two, Hansen and Lesko, were supported this summer with departmental funds. We maintain a general policy of supporting with RAs students who need to travel to CERN frequently and cannot be TAs, or who are in the final stages of their data analysis. One of our recent undergraduates M. Ambrose is now at the Science and Technology Policy Institute (STPI), in Washington DC. The graduate students advised by Mans are Klapeotke, Gude and Pastika; their graduation dates are expected to be 2013 for Klapoetke and 2014 for Gude and Pastika. Tambe, who is advised by Kubota, should graduate during 2014 and Turkewitz, also advised by Kubota is expected to graduate in 2015. Rusack is advising three new graduate students, Finkel, Hansen and Kalafut and Mans is advising another new student, Lesko. It is our practice to meet as a group most weekdays in an informal meeting with our students to discuss with them their work and to hear of their progress.

One measure of the extensive contributions that our group continues to make to CMS is the number of talks given by members of the group: this year we gave more than 490 talks at CMS meetings between August 2012 and August 2013. The group has also contributed significantly to the process of publishing results from CMS. The group has been very active in the process of shepherding analyses to publication through the CMS Analysis Review Committees (ARC). Members of the ARC assigned to a paper counsel and critique authors of a paper and generally help with the paper preparation process. Minnesota group members have collectively been on ARCs for 15 different papers. Additionally, Mans was the primary editor of the HCAL upgrade TDR and Dahmes was a

chapter editor for the same document [2].

2.2 Physics Analyses in the Recent Grant Period

2.2.1 Search for the Higgs Boson

The Minnesota group contributed to the discovery of the Higgs at LHC in the $H \to \gamma\gamma$ channel, a channel which was motivated by our long-standing involvement in the ECAL. With the first 7 TeV data from CMS, Rusack, Franzoni, and De-Benedetti worked on the measurement of the inclusive photon cross-section, which established the techniques and tools for high momentum photon analysis [3]. As the luminosity increased, the search for the Higgs became a viable physics goal and Franzoni and Rekovic led our efforts on the development of the analysis framework and the signal modeling for the Higgs search. This was a natural extension of Franzoni's work as ECAL DPG convener for two years before. This data analysis framework was used to process the data, apply corrections and obtain the key performance and analysis distributions used to extract limits and significance plots. Our contribution to the analysis was the development the tools to model the expected mass distribution for the Higgs signal, with full implementation of the treatment of its systematic uncertainties. Another contribution made by our group was an investigation of the use of photon timing in the ECAL to help with the vertex assignment and Franzoni was the author of the section on timing for the new CMS detector paper that was written as background for the Higgs $\to \gamma\gamma$ analysis [4].

2.3 Standard Model Measurements

In addition to our contributions to the hunt for the Higgs, our focus has been on detailed measurements of processes within the Standard Model. In the model the Higgs mechanism was originally motivated to provide masses to the W and Z boson. The Standard Model makes many precision predictions on how the Higgs mass and its properties are related to observables of the weak bosons and the top quark. These predictions are violated to a greater or lesser extent in the many alternative models which are nearly indistinguishable from the Standard Model in the gross-scale features of the scalar boson decays. As a result, precision measurements of both the Higgs and electroweak particles are crucial to testing the Standard Model and identifying the nature of any new physics observed.

One of the difficulties with working at a hadron collider is that the basic Standard Model couplings are overlaid with the complex structure of the target particles. With a high cross-section and clear easily-reconstructed leptonic decays, the Z boson is an excellent tool for studies of the structure of the proton and the boundary between perturbative and non-perturbative physics. By studying the distribution of Z bosons as a function of their rapidity and transverse momentum, it is possible to constrain the parton distribution functions (PDFs) as well as study QCD at high momentum transfer, a region which is quite important for high-mass searches. Mans was the lead author for the first CMS paper on the differential cross-sections as a function of Z rapidity and transverse momentum which was published by PRD in February of 2012 [5]. The Minnesota group was responsible for the full measurement in the electron channel (Mans, Franzoni, Rekovic, Haupt, Klapoetke), the combination of the electron and muon channels was performed by Mans and Pastika, and the important technique of electron reconstruction in the forward calorimeter was developed at Minnesota as discussed later.

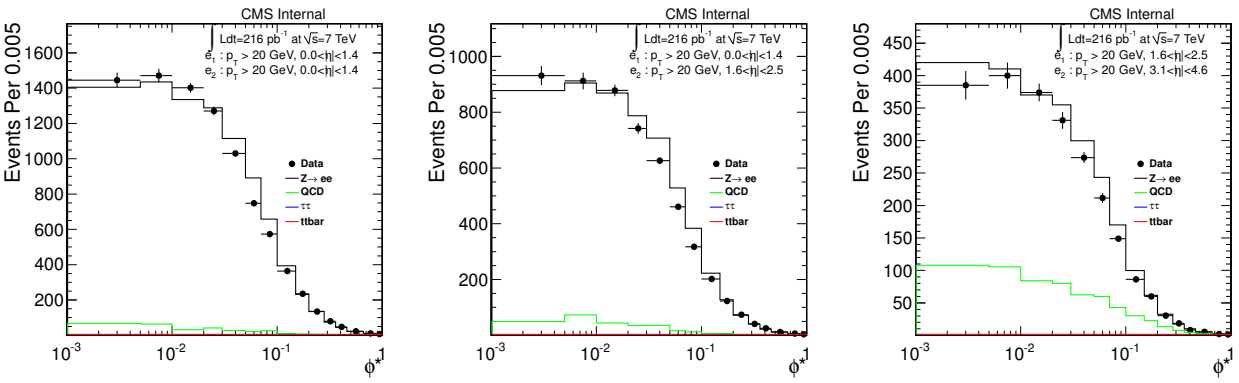

Figure 1: Distribution of ϕ^* variable for three different detector regions, corresponding to different Z rapidity ranges. The simulation results are not corrected for detector efficiency differences between data and simulation.

Since the publication of the rapidity and transverse momentum paper, the group has been working on the measurement of the differential distribution of Z bosons as a function of lepton pseudorapidity and the ϕ^* variable [6]. The ϕ^* variable enables an increase in the precision of studies that were previously made with transverse momentum analyses. The energy resolution of the calorimeters limits such studies particularly at low values of boson transverse momentum, where many questions arise in the theory. In calorimeters, it is possible to achieve higher positional resolution than energy resolution. In this way, just as transverse momentum is a refinement of 'traditional' momentum by removing the longitudinal component, ϕ^* is a refinement of transverse momentum by removing the energy component but the positional component is preserved. The ϕ^* is correlated with the ratio of transverse momentum to invariant mass, a unit-less number with most events falling between zero and one. Perturbative calculations of the differential cross section with respect to transverse momentum diverges at low values and how to handle this divergence is under debate and in need of experimental input. One method is to treat the divergence non-perturbatively by introducing a Sudakov form factor, another is to continue perturbation by re-summing the calculation in order of leading logarithms (LL, NLL, etc).

Klapoetke and Gude are working on the first measurement of ϕ^* using CMS data. The initial result, using a portion of 2011 data, is the subject of Klapoetke's dissertation. Initial plots, not yet fully corrected for detector efficiencies and reconstruction effects, are shown in Figure 1. Gude will complete a full analysis of 2011 and 2012 data and work on the CMS publication on the topic along with Ruckstuhl as she becomes familar with CMS analysis processes and techniques.

2.3.1 Search for Heavy Stable Particles as a signature for Dark Matter

One of the reasons that SUSY has been so compelling is that it provides a natural dark-matter candidate, a stable neutral particle, known as the 'Lightest Stable Particle' or LSP, which in many models is the neutralino $\tilde{\chi}_1^0$. The LSP has been searched for unsuccessfully in a large part of the accessible SUSY parameter space by searching for events with large missing transverse energies, $\not{E}_{\mathrm{T}}$. However, there remain parts of the kinematically accessible phase space that have yet to be explored; one of these is the "coannihilation strip," where, in the framework of cMSSM (constrained minimum SUSY), a semistable stau ($\tilde{\tau}$) is predicted to exist with the property that it decays to the LSP ($\tilde{\chi}_1^0$) and a τ with a long lifetime. The lifetime of the $\tilde{\tau}$ prevents LSP from being detected in

searches that rely on missing transverse energy ($\not\!\!E_{\rm T}$). Our approach is to search for $\tilde{\tau}$ directly using dE/dx measurements in the tracker system and timing measurements made in the muon system. If we find the $\tilde{\tau}$, it will provide a strong evidence for the LSP neutralino as a dark matter candidate.

On the other hand, if the symmetry breaking mechanism of supersymmetry is gauge-mediated (GMSB) [7], it is quite possible that the gravitino ($\tilde{G}$) is the LSP and the source of dark matter in the Universe. We can use $\not\!\!E_{\rm T}$ to detect the gravitinos when a pair of superparticles are produced and decay to it. When the $\tilde{G}$ mass is large enough, the next lightest SUSY particle (NLSP) could be a neutralino $\tilde{\chi}_1^0$ and will have a long enough lifetime to be detectable. Specifically, the decay is $\tilde{\chi}_1^0 \rightarrow \tilde{G} + \gamma$ with the photon delayed relative to photons from the primary interaction. In this scenario, the ECAL timing measurements can be used to find events containing $\tilde{\chi}_1^0$ and $\tilde{G}$ with higher sensitivity. Note that as the ECAL timing resolution deteriorates for particles with small energy deposit such as HSCPs, it is not useful for setting tighter limits in the absence of discovery. However, in case of discovery, the ECAL timing measurements will provide a valuable additional consistency check.

2.3.2 Search for Neutralino with Long Lifetime

In GMSB models the lifetime of the $\tilde{\chi}_1^0$ is proportional to the square of the $\tilde{G}$ mass, and can easily be more than a few nanoseconds with proper decay length in excess of $c\tau_\chi = 30$ cm. In this case, in addition to $\not\!\!E_{\rm T}$ the delayed arrival time of the γ in the electromagnetic calorimeter (ECAL) will be readily identifiable, since the timing resolution (σ_t) of ECAL is better than 400 ps, and is a powerful tool to reject a large fraction of background.

Based on about 5 fb^{-1} of data, CMS published upper limits which range from 0.04 pb at $c\tau_\chi = 30$ cm to 0.11 pb when $c\tau_\chi = 6$ m [8]. These results are based on the analysis carried out by the Rome group which assumed "Snowmass Points and Slopes 8" in the SUSY parameter space and focused on a scenario when the $\tilde{\chi}_1^0$ is wino like. These results compare favorably to the result of 0.1 pb obtained from the analysis of inclusive single photon + large $\not\!\!E_{\rm T}$ events [9]. Since we joined the effort at a late stage of the analysis, we focused our effort on devising the optimum way to utilize the ECAL timing measurements, and also understanding calibration and systematic uncertainties. This included a way to reduce the timing variation in individual events arising partially from the z position of the production vertex as well as short-term timing instability of the detector. This was accomplished by measuring the photon timing relative to the timing of the jet(s) in the event.

With the arrival of the 8 TeV data and the departure of the main personnel from the Rome group, we have taken over the entire analysis. Kao, Norbert and Kubota first invested some time devising a new set of triggers for the analysis which can be shared with the group looking for similar decays through a search for displaced converted photons. This was necessary partially to maintain the trigger rates to an acceptable level when the luminosity was increasing, and also because we wanted to have less model dependent results. In 2011, we relied on the jet multiplicity (greater than 2) to reduce the trigger rate, but this made our results dependent on the production mechanisms of neutralinos as some models predicted that they are often associated with 2 or fewer jets. Since we have to rely on $\not\!\!E_{\rm T}$ to minimize the background in our analysis, it seemed obvious to us that we should use it in the trigger, too, instead of the jet multiplicity. Because the $\not\!\!E_{\rm T}$ requirement was more effective in reducing the trigger rate than the jet multiplicity, we were able to lower the photon energy threshold from 90 to 65 GeV which is unusual.

With the larger dataset at $\sqrt{s} = 8$TeV, we found that most of the background events with delayed

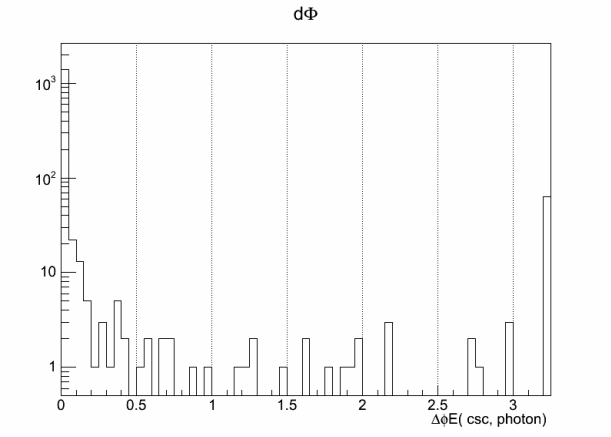

Figure 2: The difference in the azimuthal angles measured in ECAL and the muon system. The peak at zero is due to MIB background.

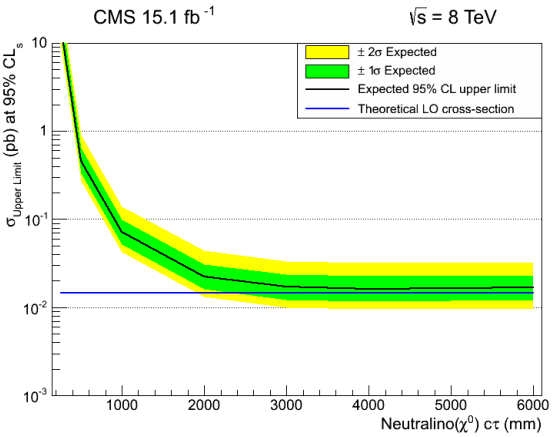

Figure 3: Expected LSP production upper limit as a function of its proper decay distance.

time measurements were due to machine induced background (MIB). *i.e.* they are due to proton beams which fell into wrong RF wave buckets in the beam. By looking at the correlation in the azimuthal angles obtained from ECAL and a track segment reconstructed in the muon system, we were able to reject most of these background. Fig. 2 shows the distribution of the difference in the azimuthal angles measured in ECAL and the muon system. The peak at zero is due to MIB. As a result, we are able to reject more than 90% of MIB background. Once the background from this source is reduced, the remaining background it estimated by the ABCD method. *i.e.* the background in the signal region (D): $t_{ECAL} > 3$ ns and $\not\!\!E_{\rm T} > 60$GeV was estimated from the background estimated in the A region ($t_{ECAL} < -3$ ns and $\not\!\!E_{\rm T} < 60$GeV), as well as the B ($t_{ECAL} > 3$ ns and $\not\!\!E_{\rm T} < 60$GeV) and C ($t_{ECAL} < -3$ ns and $\not\!\!E_{\rm T} > 60$GeV) regions because the timing measurements and $\not\!\!E_{\rm T}$ should be uncorrelated for the remaining background events.

When we require that there are at least two jets in each event to reduce QCD background, our prediction of the background in the signal region is 5.6. Based on it, we can calculate the expected upper limit on the cross section as a function of the proper decay distance we assume (which will change the efficiency for the signal neutralino to decay inside the ECAL), which is shown in Fig. 3 indicating that our sensitivity will improve as expected.

2.3.3 Search for Long-lived Stau and other Heavy Stable Charged Particles

Many models, including both SUSY and Extra Dimensions, predict a long-lived charge particle, which can be detected in CMS. The heavy stable charged particle, or HSCP as it is known, could be a $\tilde{g}$, a $\tilde{t}$ or a $\tilde{\tau}$. From the kinematics they are generally produced with a $p_{\rm T}$ that is comparable to their mass. As a result, a large fraction of HSCPs are produced with $\beta \ll 1$. Consequently their specific ionization, dE/dx, which can be measured in the tracker, and time-of-flight, which can be measured with the muon system are both significantly different from light stable standard-model particles. These differences are shown in Fig. 4. In the figure the $p_{\rm T}$ spectra (left) and a dE/dx discriminator I_as is shown for Standard Model and for different HSCP masses.

The search for HSCP in CMS is a multi-university project. Cooper and Kubota contributed to the estimation of the systematic uncertanties arising from the dE/dx measurements using a sample

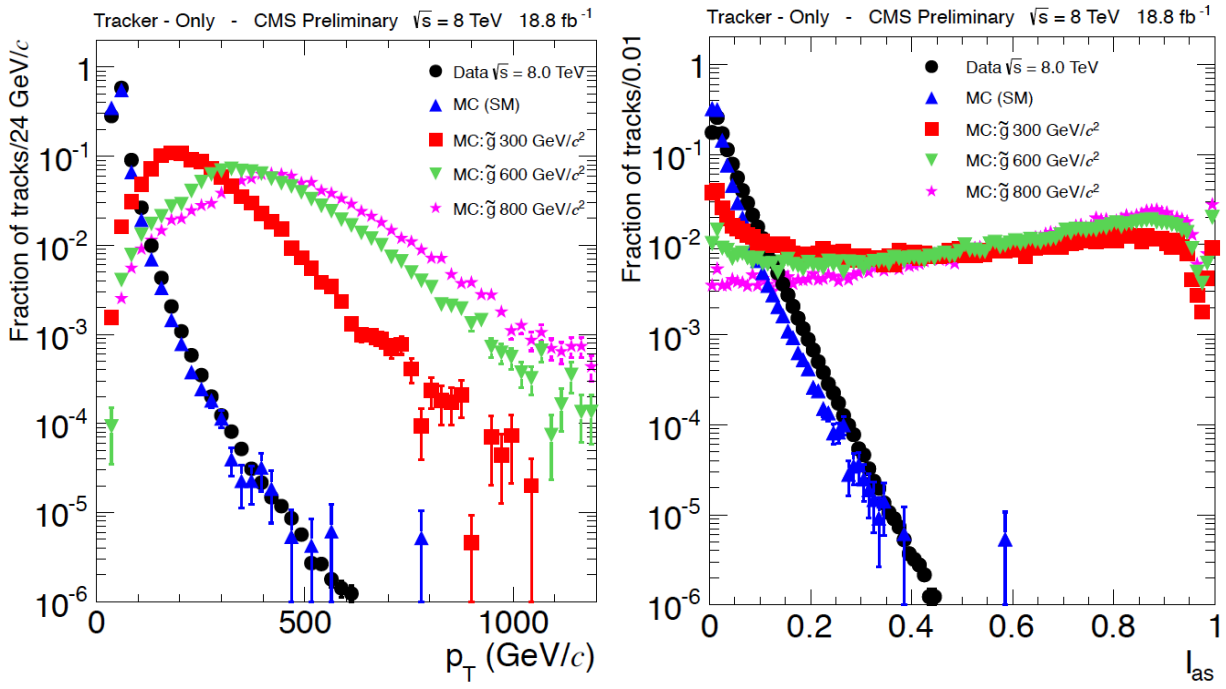

Figure 4: Distributions of p_{T} (left) and dE/dx discriminator (right: see text for definition) for data and signal Monte Carlo.

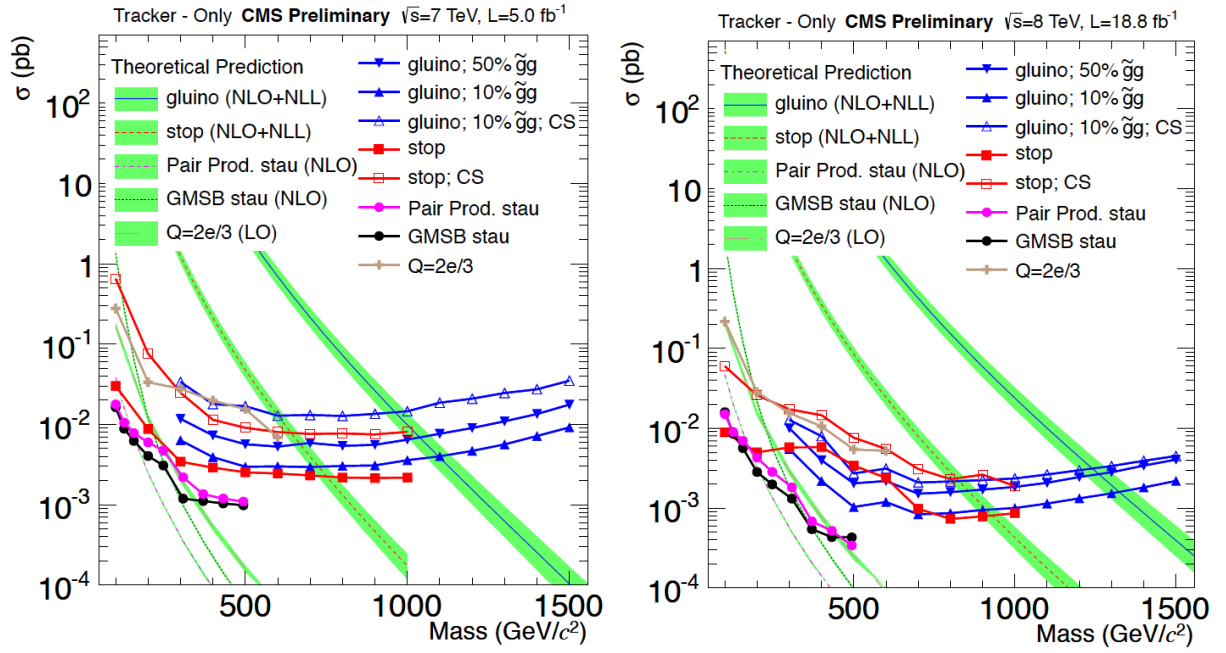

Figure 5: Cross section limits for gluino, stop and stau as a function of mass, and predicted cross sections for $\sqrt{s} = 7$ and 8 TeV.

of protons. They also carried out the 2nd statistical analysis of the data based on the shape of the dE/dx distributions and confirmed the primary analysis which used a simpler "cut and count" technique. Seth Cooper wrote his thesis based on the shape-based analysis and demonstrated that if a signal was found, his analysis would be able observe a 5 σ effect with up to a factor three less data for highest mass gluino and other HSCP models. However, the limits are comparable in the absence of signal to the "cut and count" limits. Our analysis served as a confirmation of the measurement of the upper limits shown for the two datasets [10],[11] in Fig. 5. Assuming the standard HSCP production cross sections for gluino, stop and stau, we have set lower mass limit for gluino of about 1300 GeV, stop of about 900 GeV, and stau of 435 GeV assuming the GMSB model and 339 GeV for pair production[12]. Jared Turkewitz has repeated our analysis for the 8 TeV data, and confirmed the primary analysis results. The gains in the signal sensitivities are still better than the "cut and count" analysis.

2.4 Search for Heavy Right-Handed Neutrinos and Charged Gauge Bosons

Despite its many successes, the Standard Model has more than a few peculiarities that are not well motivated. One such instance, the maximal violation of parity in Weak interactions, implies that the process $W^+ \to \mu^+\nu_\mu$ can only proceed via left-handed particles and right-handed anti-particles. This forces neutrinos to be left-handed and massless, in contrast to the experimental evidence for massive neutrinos.

The parity violation of the Standard Model is manifestly required by experiment at low energy scales, but it has been an open question for years if parity symmetry might be restored at a higher scale. The Left-Right symmetric extensions to the Standard Model that restore this symmetry explain parity violation as a spontaneously broken symmetry. Such extensions assume the existence of a right-handed weak-sector, complete with heavy charged ($W_R^\pm$) and neutral gauge bosons, and right-handed massive neutrinos N_ℓ ($\ell = e, \mu, \tau$). The very light mass of the left-handed neutrinos in the Standard Model can then be understood through the seesaw mechanism. Indirect searches have constrained the mass of a W_R boson to be larger than 2.5 TeV. Direct searches at the Tevatron have established a lower limit of nearly 800 GeV.

The Minnesota group (Dahmes, Mans, and Pastika) searches for LR signatures via the decay $W_R \to \ell N_\ell \to \ell\ell W_R^* \to \ell\ell qq'$, where $\ell = e, \mu$ and the quarks are reconstructed as jets in the detector. Due to the expected mass of the W_R boson, the final state leptons (electrons or muons) and jets are produced with large transverse momentum. As a result, the Standard Model background processes in this search, primarily $t\bar{t}$ and Drell-Yan + jets processes, produce real high-p_T leptons and jets in the final state. In our previous search for $W_R \to \mu N_\mu$ signatures using 5 fb^{-1} of 7 TeV data, which was recently published [13], we excluded W_R bosons with mass less than 2.5 TeV depending on the assumed mass of N_μ.

In 2012, we added the $W_R \to eN_e \to eeqq'$ decay mode, which had previously been studied by INR (Moscow), at the request of CMS management so that the results from this high-priority analysis could be ready for ICHEP. For this round of results, we added Franzoni, Kubota and Turkowitz to the analysis team and using 3.6 fb^{-1} of 8 TeV data collected through June 2012, we searched for W_R signatures in both channels and presented our results at the ICHEP conference in July 2012. We found no evidence for W_R production in either the electron or muon channel.

Since ICHEP, we have completed the paper on the 7 TeV limit in the muon channel. Dahmes, Mans, and Pastika have extended the search for W_R production using the full 19.6 fb^{-1} of 8 TeV

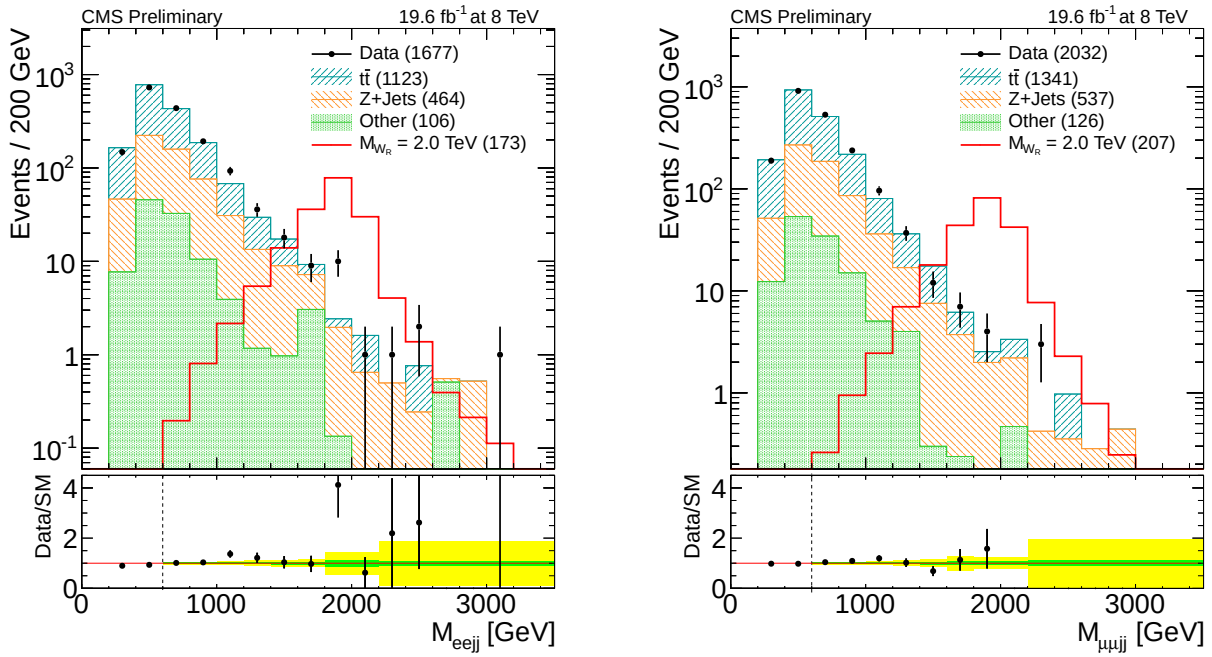

Figure 6: Mass distribution for events from the electron (left) and (muon) channels passing all the selections (points with error bars), with hatched stacked histograms showing the background components. The signal mass point $M_{W_R} = 2000$ GeV, $M_{N_\mu} = 1000$ GeV, is included for comparison (open red histogram). The number of events from each background process (and the expected number of signal events) is included in parentheses in the legend. The data is compared to Standard Model expectations in the lower portion of the figure. The total background systematic uncertainty (yellow band), and the background uncertainty after neglecting the uncertainty due to background modeling (green band), are included as a function of $M_{\ell\ell jj}$ above 600 GeV.

pp collision data collected in 2012. We present the four-object mass distribution ($M_{\ell\ell jj}$) in Figure 6. We find the data to be in good agreement with Standard Model expectations for the muon channel. We observe a small excess near $M_{eejj} \sim 1$ TeV in the electron channel, although the size of this excess is too small to be explained by strict left-right symmetry. Due to the increased LHC collision energy in 2012, and the wealth of data collected, we expect to increase the exclusion in the (W_R, N_ℓ) mass plane to roughly $M_{W_R} = 3$ TeV using the available 8 TeV data. The W_R search will be the basis for Pastika's disseration which will also include the published results for hadronic decay of a W_R to establish a full view on the W_R question for the LHC Run I era. This work is expected to be completed before the end of current funding period.

While the Minnesota group is motivated by the search for right-handed neutrinos and weak bosons, the analysis is intentionally designed to apply a minimum set of requirements on the dilepton plus dijet event topology. As a result, the results of the analysis can be applied to many models which predict a massive resonance with a branching fraction into a lepton pair and a jet pair. We are discussing with colleagues in theory to identify specific models for consideration.

2.5 Reconstruction and Calibration Efforts in the Recent Grant Period

As a group of experimentalists we believe it is important to address our physics goals through both building instruments and analyzing the data from them. The development of new reconstruction techniques, detector calibration strategies, and triggers is a crucial "construction" effort which we connect directly to our data analysis and physics goals.

2.5.1 Forward Electron Reconstruction and Triggering

To allow the largest acceptance for Z physics studies, the Minnesota group has developed a set of techniques for the reconstruction and identification of high p_{T} electrons in the forward hadron calorimeter (HF), which covers the high η regions ($3.0 \leq |\eta| \leq 5.0$). The HF detects both electrons and jets using a monolithic calorimeter design with a steel absorber and quartz fiber as the active element collecting Čherenkov light from shower particles which pass through the fibers. Over the last three years, several members of the group and visiting undergraduate researchers have developed the basic reconstruction techniques and then enhanced these techniques to manage the rising luminosity of LHC.

Klapoetke has been the primary developer of the HF electron reconstruction code, which was developed and proven entirely by the Minnesota group under the leadership of Professor Mans. In the summer of 2011, Frye, an REU student, improved the definition of the longitudinal shower-shape variable to correct for the logarithmic increase in electromagnetic shower depth with energy. To allow the acquisition of these events in the high-luminosity environment of LHC, Gude and Schroeder, under the direction of Dahmes, have developed Level 1 and High-Level Triggers for Z bosons with an electron in HF. Gude has also extended his effort to the region of ECAL without tracker coverage, an area discussed in more detail below.

With the increased luminosity of LHC in 2011 and 2012, the number of overlapping interactions (pileup) has greatly increased. Given its large cell size (0.17 x 0.17), the HF has been particularly affected by the high pileup. Klapoetke has developed new, more robust techniques for correcting the energy of HF clusters as a function of pileup, while Gude has optimized the triggers to increase their robustness against pileup and developed pileup-dependent corrections for the identification variables used in the reconstruction of forward electrons. A dielectron mass distribution showing the clear Z peak above background is given in Fig. 7.

2.6 Calibration of the HF Calorimeter

The Minnesota group has also made significant contributions to the operation of the hadron calorimeter through the development and implementation of the Z→ee calibration for the forward detector. The Z signal in the forward calorimeter, as identified using the Minnesota algorithms, is clean and relatively background-free. This technique is the primary calibration for the absolute HF energy scale and the eta-dependence of the calibration. The calibration uses the position of the cluster in HF along with the energy and position of the second electron as measured in the ECAL to predict the energy of the electron in HF. This energy is compared with observed energy to enable the calibration. The calibration is performed ring-by-ring at constant ieta value, requiring a pre-calibration by phi-symmetry, which has been done. Other work by Hanson (undergraduate) has provided corrections for pileup effects and Mans has also developed a Monte Carlo-driven technique to obtain a calibration for the short fibers of HF. The results of these two calibrations have been

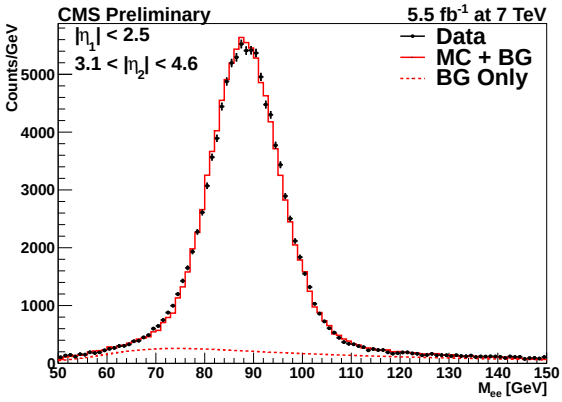

Figure 7: Dielectron mass distribution near the Z peak for events with an electron in the forward calorimeter for the full 2011 dataset.

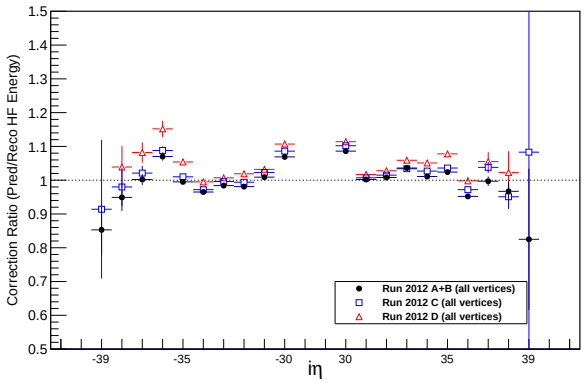

Figure 8: HF η-dependent calibration results for the data-taking periods of 2012.

applied for all 2012 data-taking with HF, providing the first truly calibrated data from the HF detector.

The calibration is particularly valuable as it is well-defined physically and can be maintained in future years. Currently, Dahmes has taken the task of improving the documentation and workflows for the calibration and carrying out studies on the calibration for 2012 and preparing a paper documenting these calibration techniques. A plot of the calibration factors for 2012, split by data-taking period, is shown in Fig. 8. As the full set of phototubes will be replaced on HF during the current shutdown, it will be necessary to re-establish the detector's calibration baseline quickly in 2015. The group is automating the process as much as possible to make this effort efficient.

2.7 Electron Identification and Calibration of the Forward ECAL

The Minnesota group, having developed electromagnetic particle identification for HF, is now leading the effort to fully qualify the forward portion of the crystal calorimeter for electron reconstruction. The region of the electromagnetic calorimeter beyond $|\eta| = 2.5$ is currently unused for electron-based analyses. However, 10% of H$\rightarrow$ ZZ$* \rightarrow$ ee$\ell\ell$ events have an electron into this region. Also, significant numbers of Z bosons have decay electrons in this region as well. For data taking in 2012, Gude developed a trigger to select these events. Finkel, under the direction of Mans and Dahmes, has been developing identification criteria for the forward electrons and studying the differences between data and simulation.

Finkel has found a very clear Z peak in the data, with significant disagreements between simulation and data which point to 4-10% miscalibration effects in this portion of the endcap ECAL as can be seen in Fig. 9. This portion of the detector has been calibrated only using original construction information, muon "splash" events, and ϕ symmetry considerations. The ϕ-symmetry calibration has significant systematic difficulties as the crystals are on a Cartesian grid rather than an $\eta - \phi$ grid. Under the direction of Rusack, Finkel has implemented a calibration based on the Z events which improves the Z peak dramatically as seen in Fig. 10. To produce this figure, the full 2012 data set was split into two samples, alternating subsamples between each event so that the two samples

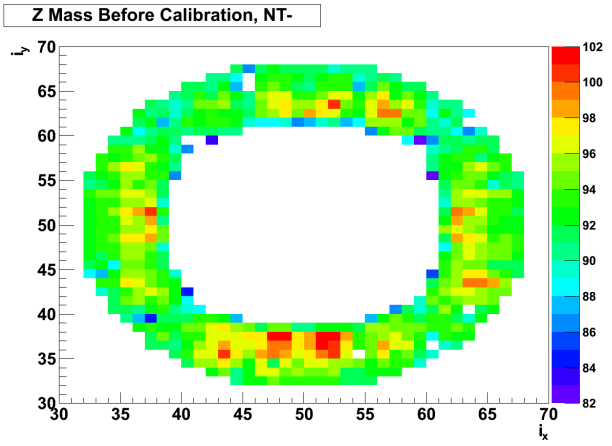

Figure 9: Z mass fit peaks before calibration in the negative ECAL endcap, for each crystal.

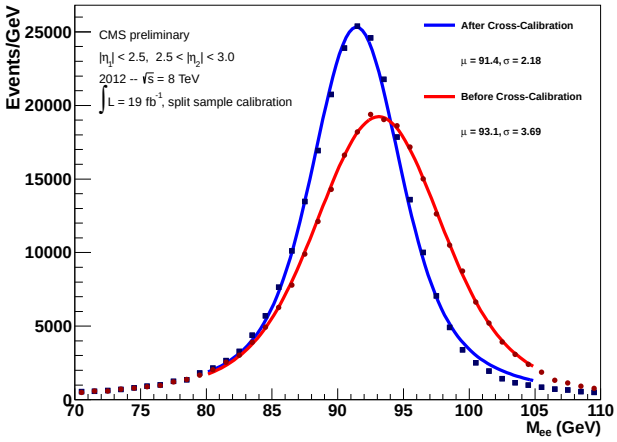

Figure 10: Calibration results for the trackless region of ECAL based on Minnesota work.

have the same exposure to detector and luminosity changes. One sample was used for calibration and the second was used for validation and to make the plot shown. The fits are to a Voigt function, with the Lorentzian width fixed to the physical Z width and the Gaussian widths shown on the figure.

The cleanliness of this sample shows how effectively this region can be used for rapidity and forward-backward asymetry measurements allowing minimal acceptance corrections and theory uncertainty in the measurement.

2.8 ECAL Timing Calibration

Another detector-related development of the Minnesota group which has had a direct impact on the physics efforts of the group has been the precision timing calibration of the 72,000 ECAL crystals. The fast PWO scintillation light and the electronics pulse shaping allow an excellent time resolution to be obtained for the ECAL. The group is responsible for delivering the timing calibration constants to the collaboration.

Individual channel synchronization stability at the 1 ns level is required to ensure good amplitude reconstruction since a timing difference of 1 ns causes a bias of approximately 0.1% on the reconstructed amplitude. The signal timing is also used in the reconstruction phase to reject anomalous signals, and out-of-time pile-up energy deposits (a cut on the signal timing of 3 ns is used for this purpose). We use the timing performance of the ECAL directly in the search for long-lived particles decaying into photons described above.

Kubota and his graduate students have developed a method to achieve a further level of time alignment in the offline reconstruction by using single-crystal additive calibration constants measured from data. The algorithm used employs ratios of consecutive samples. In this method only hits in events with loosely defined electrons or hadronic activity are used, and they are required to be part of a cluster with $E_{\mathrm{T}} \geq 2$GeV and a time within 5 (7) ns of zero in EB (EE). The single crystal calibration constants are then set to compensate for any residual shifts observed. The time calibration has been adjusted several times during the 2011 and 2012 runs to account for both global phase changes induced by drifts of the CMS clock relative to the LHC bunch crossings and

localized de-synchronizations due to hardware interventions on the read-out electronics.

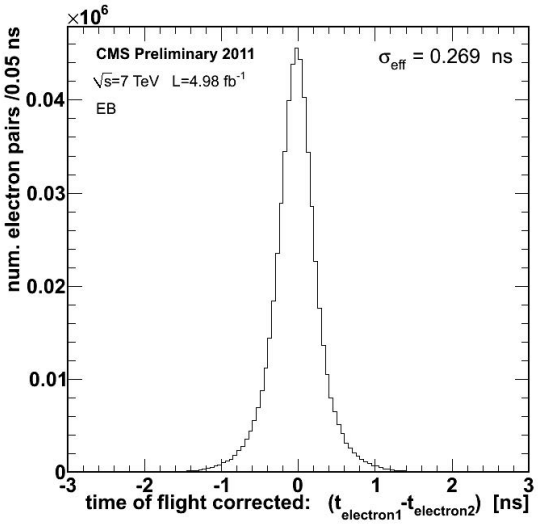

Figure 11: Difference between the time of the electron and positron signals in decay.

Figure 11 shows the difference between the reconstructed times of the most energetic hit of either electron in Z decay. The impact of the finite duration of the bunch crossing cancels in the difference, as well as global phase shifts. The widths of the distributions are 269 ps and 400 ps for the barrel and endcap, respectively. Most of the ECAL timing use for physics involves timing differences between two physics objects in a given event, therefore the above timing resolution is a good indicator of the ECAL timing measurement potential. In particular, the time resolution for a single ECAL channel is found to be 0.19 ns and 0.28 ns in the EB and EE respectively for the energy range of electrons from Z decays.

2.9 Long-Term Performance of the Electromagnetic Calorimeter

As it is known that the $PbWO_4$ crystals of ECAL will experience permanent unrecoverable damage with hadronic radiation, CMS initiated a study of how the performance of the calorimeter will change with different levels of degradation. This study was led by Singovski, a project-supported engineer, and Rusack, with contributions by graduate student DeBenedetti and several Minnesota undergraduates. Hadron damage in the crystals is caused by the creation of color centers that absorb the scintillation light by hadrons interacting with the nuclei, either through fission of spallation processes, and creating non-recoverable defects. The mechanism is discussed in more detail in a study that Singovski and Rusack conducted in 2012 with a group from Minsk on irradiation damage in crystals [14]. In ECAL the effect is worse in the high η regions of the endcap calorimeters, where the damage will be significant, than in the barrel calorimeter, where the changes will be small.

With the plan to extend the running of the LHC with the High-Luminosity LHC with a factor of ten increase in the total delivered luminosity, this question became urgent in the past year as we evaluated the necessity of replacing the endcap calorimeters.

Between 2009 and 2012 twenty-seven crystals with the endcap geometry were irradiated with doses between 10^{13} and 10^{15} protons/cm^2 in the PS. After the irradiation at least six months were required

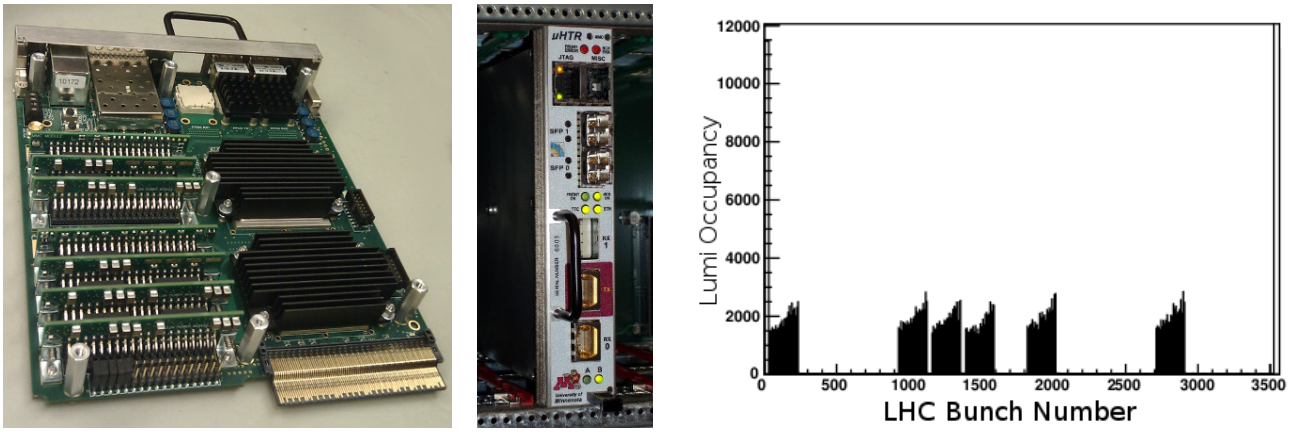

Figure 12: (Left) Photographs of the top and front of a prototype uHTR produced at Minnesota (Right) Image of the luminosity histogram acquired by the uHTR during p+Pb running of the LHC in early 2013.

before they could be safely handled and, once cool, they were assembled into a 5×5 test matrix, and the resolution and linearity were measured in the H4 test beam at CERN. Using data collected with different sub-matrices of crystals with different degrees of degradation, we were able to extrapolate the changes in the performance with hadron flux. It was found that after 5×10^{13} protons/cm^2 - the total hadron flux expected at the highest η's of the calorimeter - the stochastic term will increase from $3.5\%/\sqrt{(E)}$ to $\sim 12\%/\sqrt{(E)}$ and the constant term can be expected to increase from 0.5% to 5%. The study was written up in a CMS detector note [15]. The results obtained were consisted with optical simulations performed with Litrani and GEANT4, thus confirming our ability to predict the long-term performance of the detector.

It was based on the results of these tests and the assurance that our simulations were providing accurate predictions, that the decision was made to remove the endcap calorimeter for the HL-LHC and to replace it with a more robust detector.

2.10 Phase 1 Detector Upgrades

2.11 HCAL Phase 1 Upgrade

Over the last three years, the Minnesota group has lead the development of the readout electronics required for the upgrade of the hadron calorimeter. The first sections of this upgrade will be installed during the current LHC shutdown and will begin yielding physics benefits with the new run. Besides the management roles of Mans and Kubota in the upgrade (L2 for HCAL and L3 for HCAL backend, respectively), the Minnesota group is responsible for the development of the uTCA HCAL Trigger and Readout card (uHTR). The uHTR is responsible for receiving data from the front-ends at a rate three times faster than the existing electronics, for calculating the HCAL trigger energies and transmitting them into the calorimeter trigger, and for maintaining the buffer of data waiting for the decision of the trigger. The card has been under development for several years by Mans and Frahm, an engineer supported by the Upgrade R&D program and now the LHC CMS Upgrade Project. The full prototype has been recently completed and photographs of a completed card are shown in Fig. 12.

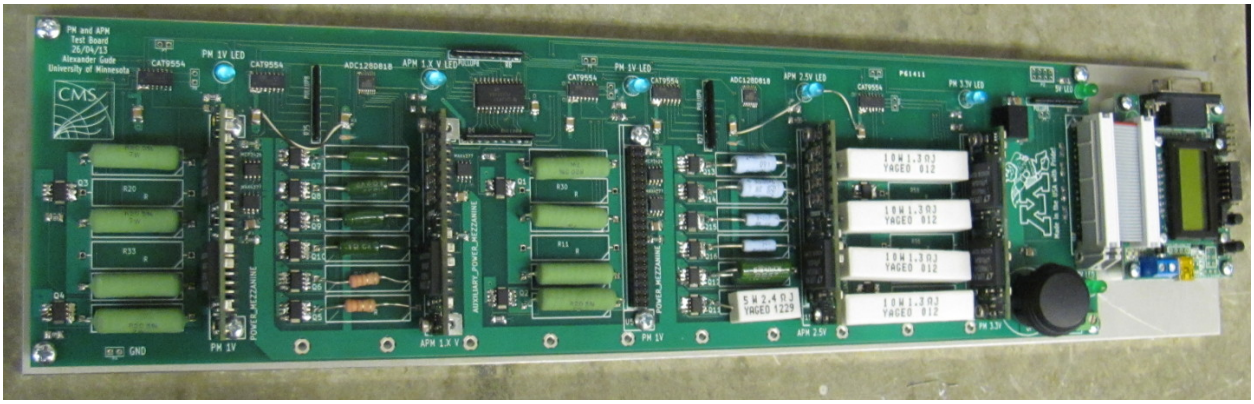

Figure 13: Photograph of the uHTR power mezzanine tester capable of testing five power mezzanines simultaneously (enough for a single uHTR). In the photograph, four mezzanines are loaded with the middle test site empty.

One of these cards has been tested during the p+Pb running of the LHC in February 2013 using optically-split fibers. With this test, and tests of previous R&D prototype cards, the primary set of required functionality has been demonstrated. This includes DAQ as well as the acquisition of luminosity data as seen the right of Fig. 12. Kao has been responsible for the development of all the software related to the readout and testing of the prototype cards and for the initial development of the luminosity readout system which will now be a joint effort with the CMS Luminosity group.

A few minor issues were identified with the prototype cards which have been corrected in the pre-production cards now under manufacture by the Kolkata group in India. Beyond the leading work from Kao and Frahm, other members of the Minnesota group have become involved as the production of the cards comes closer. Gude has designed and constructed a test fixture for testing and burn-in of the DC-DC mezzanines of the uHTR shown in Fig. 13. Pastika has provided the software for this test fixture as well as a previous smaller test fixture, while Norbert is developing a fixture for the pre-programming and checkout of the other mezzanines required by the uHTR. The preparation of these test fixtures will accelerate the delivery of correct and functional uHTRs.

The group is not only developing the hardware, but also leading the effort to integrate the benefits into CMS data taking. The first benefit of the upgraded electronics will be the ability to define much more selective L1 triggers for events with electrons in the forward region.

The original design of the trigger used primitives covering large regions in $\eta - \phi$ space in the trigger chain, while the upgrade will allow flexible use of tower-level granularity. Large primitives are particularly inappropriate for electrons and low-p_{T}jets in the HF, as showers in HF are quite narrow due to the Čerenkov technology used. We are developing the hardware and HLT algorithms to take full advantage of this upgrade and to improve jet triggering as well. This work will be an important task for several of the graduate students in the group including Gude and Lesko. This effort will directly improve the data samples available for our precision electroweak measurements and is a typical example of how the group synthesizes data analysis, hardware, and detector calibration efforts to achieve our physics goals.

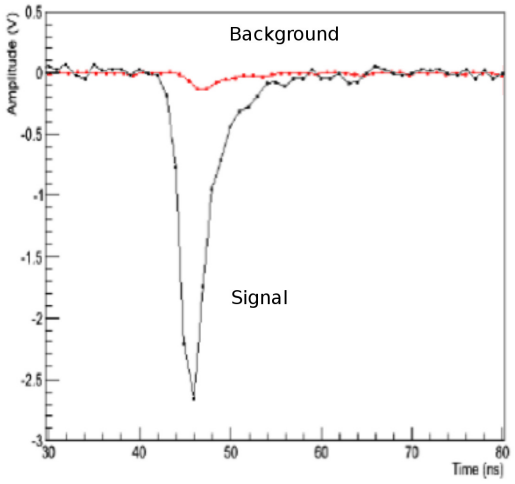

Figure 14: Typical signals seen when a proton passes in the forward direction (black) and backward direction (red) in the beam halo monitor.

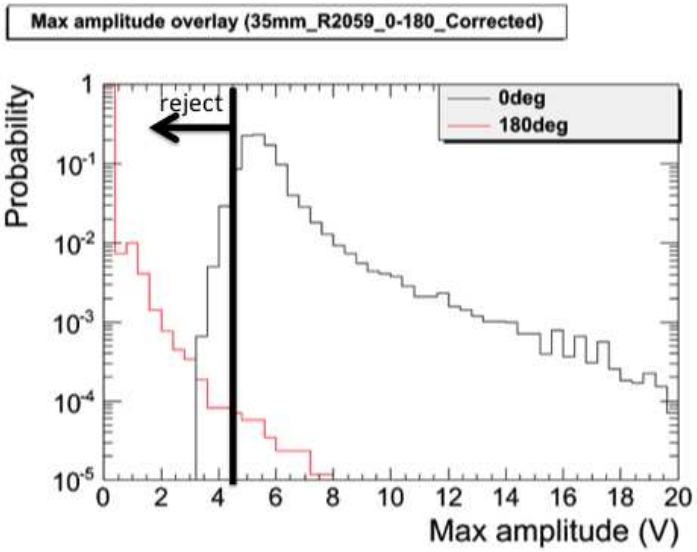

Figure 15: Rejection and selection efficiencies for backward and forward going particles.

2.12 Beam Halo Monitors

Another upgrade for the CMS detector to which the Minnesota group has contributed is the introduction of new detectors designed to detect and measure beam loss particles at a radius of ~ 2.2 m from the beam. These Beam Halo Monitors (BHM) will provide online monitoring of the beam-induced background at high radius for each bunch crossing and integrated over short time intervals (Lumi sections). They provide supplemental information to BCM-1F detectors that measure the backgrounds at small radius and have no overlap with the muon detectors. Beam halo events are a leading background for the delayed-photon search for dark matter which is led by the Minnesota group and the new detectors should improve our understanding of this background.

The technical challenge of BHM is to be able to measure small changes in flux of muons in a 'background' that is four orders of magnitude higher generated by the beam-beam collisions. To achieve this, CMS is using a method proposed by Rusack which employs a 51 mm-diameter quartz bar, blackened at one end and readout with a UV-sensitive PMT at the opposite end. This technique applies the strong directionality of Čerenkov light production, and two test beam measurements conducted at the CERN PS in 2012 have demonstrated the excellent selectivity of this tecnique. Figure 14 shows typical pulses for a forward going particle (black), and the greatly suppressed signal when the particle is propagating away from the PMT(red). The measured rejection of the signal is shown in Fig. 15.

As the signal is Čerenkov light, the pulse length is short and was measured in the test beam using the Hamamatsu PMT R2059 that will be used in the final detector to be 3.5 ns, FWHM. This effect is taken into account when the location of the detector was selected to be 20.6 m away from the IP. At this point there is a time separation of 12.5 ns between $\beta = 1$ particles from the LHC beam and from the IP. When the LHC is operating normally the MIB signal at this radius is about 1 Hz/cm^2. There will be 20 detectors placed in a ring at each end of CMS each with a surface area of 20.4 cm^2, giving a signal of approximately 20 Hz/detector under normal beam conditions.

To readout the detectors we will use the same uTCA HCAL Trigger and Readout card (uHTR)

discussed above, and the QIE10 front-end readout that will be used for the readout of the HF calorimeter and the upgrade of the CMS hadron calorimeter. As this is already a major project undertaken by our group, we profit from the synergy of the two readout schemes.

The project successfully passed a CERN Engineering Design Review in August 2013. In the near future we will test the final detector structure in the FNAL test beam and install and commission the detectors in the LHC in 2014 before LHC operations recommence. Members of the group who have contributed to this effort are Rusack, our undergraduate Ambrose in 2012 and Hansen. Ambrose did much of the test beam data analysis and simulation work for this project, and Hansen has worked on the uTCA readout, including a three week stay at CERN this summer.

2.13 Phase 2 Detector Upgrades

CERN is planning to upgrade the LHC to reach luminosities well beyond the design of 10^{34}Hz/cm^2 with the HL-LHC. CMS has embarked a detailed study of the changes that are required to be made to the detector to be able to study the physics that will become accessible at this new luminosity regime.

We see this as an opportunity to extend our research into areas beyond those accessible at the LHC, and we have taken a leadership role in this process, with Rusack as one of the two co-conveners of the Forward Detector Upgrade Working Group (FDUWG). The FDUWG is responsible to develop plans for the detector upgrade of the forward region for a Technical Proposal to be submitted to the CERN LHCC in fall 2014. In addition to this contribution, Dahmes is leading a study of the non-SUSY exotic signatures and working with Rusack to evaluate possible new detector options for CMS. Kalafut spent the summer 2013 at Fermilab working with F. Chlebana on the the problem of simulating the detector performance at the HL-LHC.

The integrated luminosity of the current LHC program (Phase 1) expected to be 500 fb^{-1}, while for the High-Luminosity LHC (Phase 2) the integrated luminosity will be 3000 fb^{-1}. The measurements that will be made possible with this increased luminosity are of very rare processes, like the triple Higgs coupling, or high-precision measurements which require high statistic, for example the branching fractions of the Higgs. Furthermore, as the Higgs was first introduced to solve the apparent breaking of unitarity in VV scattering, it is important to study VV production to understand if there are other physics processes that contribute to the restoration of unitarity in VV scattering. For this the ability to isolate VV scattering by detecting and triggering on vector-boson fusion (VBF) dijets will be essential

It is now accepted by the collaboration that the two forward calorimeters (EE and HE), as well as the preshower detector, will suffer from significant radiation effects and will need to be replaced in the shutdown before the start of HL-LHC operations (LS3). The challenge then is how to make best use of this opportunity to design and build the optimum detector system to work in this harsh environment.

2.13.1 Calorimeter Options

Much of Rusack's research effort in the past year has gone into the problem of how to build a calorimeter that will meet the highly demanding performance requirements at the HL-LHC. The pileup at the HL-LHC is expected to be on the order of 140 events for every 25 ns bunch crossing, leading to a particle flux of $\sim$ 1000 minimum ionizing particles per unit of $\eta - \phi$ space. In this

background and the compressed space of the forward region, we need to isolate and measure the energy and position of individual photons, leptons and jets. Moreover, as the large flux will activate and damage the detector materials, the components of the detector will need to be stable under irradiation up to levels of 10^{15} neutrons/cm^2, making this is an unprecedented detector challenge for our field.

Rusack is a member of the CDRD collaboration, lead by Profs. B. Cox and R. Ruchti, looking into this question. With funding from this source, the Minnesota group are investigating the possibility of using Silicon Carbide APDs to readout Čerenkov radiation. We have made in the Minnesota Nanotechnology Center a series of small APDs that we will test in the coming months, and we have also irradiated devices from GE and from Prof. J. Campbell of the University of Virginia, Electrical Engineering Department with 26 GeV protons at the CERN PS.

One of the calorimeter options proposed by the CDRD collaboration is to build the calorimeter in a 'Shashlik' geometry with small plates of LYSO as the active medium. Light is collected through quartz capillaries and brought to photodetectors. A test matrix is being built for beam tests at the Fermilab test facility. For this the readout will be identical to the HCAL upgrade readout, discussed in the Phase 1 section and Minnesota's contribution to this effort will be the uTCA board to readout the QIE and the data acquisition software.

In his function as co-convener of the FDUWG, Rusack initiated a series of discussions with members of the CALICE collaboration to investigate the feasibility of using the technique that they had developed for the ILC/CLIC communities known as the 'Particle-Flow-' or '3-D-' or 'Imaging-' calorimetry for the HL-LHC. Particle-flow calorimeters are calorimeters where individual sampling layers are highly segmented and readout independently, so that a three-dimensional image of the showers inside the calorimeter can be reconstructed.

For the CMS application we are investigating using for both the electromagnetic and hadronic sections Gaseous Electron Multiplier (GEM) chambers [17] or Micromegas [18], which are low-cost gaseous detectors developed for high rate tracking, capable of detecting single particles at rates of 1 MHz/mm^2. GEM detectors and Micromegas were developed in the framework of the RD51 project and planned for use in the upgrade of the CMS muon system and the ATLAS muon systems, respectively. The technical challenges to be addressed are, however, formidable, but we believe that recent advances in ADCs, high-rate data transfer, and high-performance FPGAs, which will be needed to form the trigger, will make this real possibility for CMS. Currently a small international collaboration with groups from both Europe and the US has formed to pursue this approach and Minnesota plans to work on the technical design, hardware development and the simulation software.

Another technical challenge that needs to be faced is the reconstruction. We are assuming in our design that there will be about 28 (38) independent layers with an average size of 7.5×7.5mm^2 (30×30mm^2) in ECAL (HCAL). Every event will produce an To reconstruct the jets is a major software task that has been addressed in the CLIC/ILC communities. We discuss below simulation efforts that Minnesota has undertaken to address this problem.

2.13.2 Phase 2 Detector Simulation

To investigate if an extension of tracking coverage from $|\eta| = 2.5$ to 4.0 would provide large benefits in the Phase 2 upgrade, Dahmes has used the Delphes fast simulation package [19] to study improvements to jet-tagging in VBF Higgs events at high luminosity. He determined the improvements

gained by extending the tracker coverage by assuming that jets could be associated with a given collision vertex if they were within the tracker acceptance. They could then be associated with a VBF jet, or associated with a separate collision vertex and removed from the analysis. The remaining jets detected in the calorimeter, but outside of the tracker acceptance, remain and contribute to background. The standard CMS analysis requirements used in VBF searches for the tagging jets were applied and the results are presented in Figure 16. Results obtained with the current tracker acceptance are shown in the left plot, and with the extended tracker acceptance in the right plot. As can be seen the rejection of pile-up jets is greatly improved with the tracker extension, as is the purity of the VBF jet sample.

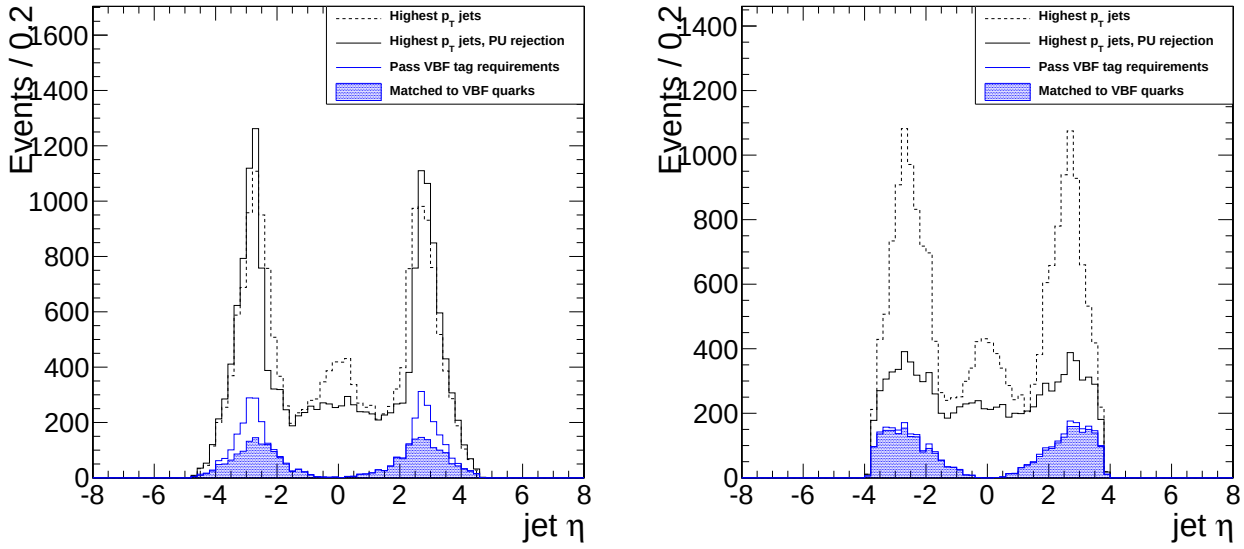

Figure 16: Pseudorapidity distribution for the two leading jets in VBF-produced Higgs events, where Higgs decay products are omitted from the jet list. In addition to the Higgs decay, an average of 140 pileup collisions are included for each event using the Delphes simulation toolkit. The CMS tracker acceptance is set to $|\eta| < 2.5$ at left and $|\eta| < 4.0$ at right.

The FDUWG team has carried out a second study to investigate the use of the advanced algorithms developed to reconstruct the complex events in Particle Flow calorimeter, in particular the Pandora framework developed initially for the CLIC collaboration [20]. Dahmes and CERN collaborators have investigated the reconstruction of HL-LHC events generated with the official CMS generators in the *ILD* detector, which in many respects is similar to CMS. They are working to adapt software designed for linear collider studies for use with pp collision events. Recently, 14 TeV $pp \to WH$ physics events have been successfully overlaid with pileup pp collisions, as shown in Figure 17. This progress will provide the opportunity to test PF Calorimeter performance in a high pileup environment as an initial step before undertaking the task of including it in the CMSSW framework.

As introduced above, Kalafut spent the summer of 2013 as an LPC fellow at Fermilab working with F. Chlebana to further develop and apply the Delphes simulation tool for the simulation of the performance of the detector in the HL-LHC environment. To provide a solid baseline for the Delphes studes, Kalifut has been comparing a Delphes model of the current detector to the results of the full Geant-based simulation of the detector. The VBF Higgs production, was used for this, with the Higgs decaying to taus as the benchmark signal $pp \to 2jets + H \to \tau\tau$. Delphes jet reconstruction will be validated once the reconstructed jet p_{T} and η distributions from Delphes

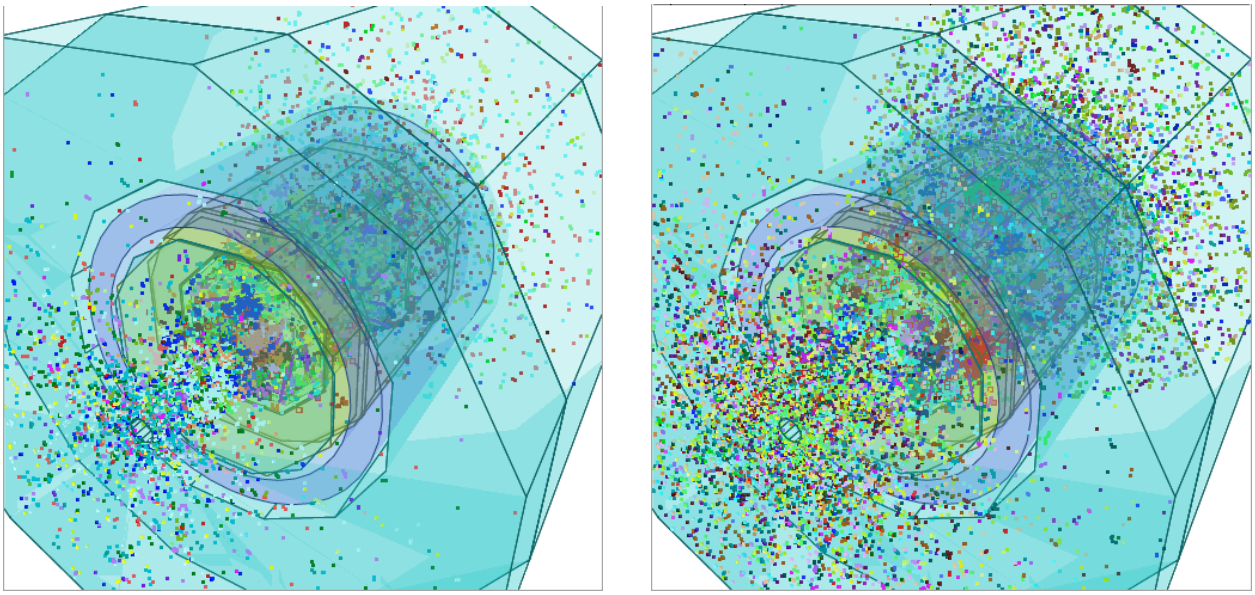

Figure 17: Event display of pp collisions simulated and reconstructed in the ILD detector. At left (right), no (20) additional pileup collisions are included along with the 14 TeV $pp \to WH$ ($W \to \ell\nu$, $H \to b\bar{b}$) event. The Higgs and pileup events were generated within the official CMS software framework and propagated through the CLIC/ILD framework.

agree with the reconstructed distributions from Geant. At present the match is excellent in the p_{T} distributions, even when the pileup is 140. However, the jet reconstruction of the fully simulated events at very high pileup shows some anomalous behavior, probably caused by failure in high background events of the clustering algorithms. Once Delphes jet reconstruction is fully validated, it can be used with increased confidence to investigate how different phase 2 detector upgrades benefit the physics measurements.

3 Physics at the Cosmic Frontier: SuperCDMS Dark Matter

3.1 Personnel

Faculty: Professors Priscilla Cushman and Vuk Mandic
Adjunct Faculty: Angela Reisetter (Evansville University)
Senior Research Associates:
Anthony Villano (50% support under NSF Integrated Tools for Underground Science)
Hassan Chagani (partly supported by SuperCDMS Project and GEODM)
Visiting Postdoc: Elias Lopez (University of Madrid, MultiDark CDMS member)
Graduate students:
Scott Fallows (est. PhD Summer 2014)
Tom Hofer (est. PhD Spring 2015)
Mark Pepin (est. PhD Fall 2015)
Allison Kennedy (est. PhD Summer 2016)
Department-supported Graduate Students: Hannah Rogers, D'Ann Barker
Graduate students expected to graduate in 2013: Jianjie Zhang
Undergraduates: Alex Codoreanu, Christopher Phenicie, Deano Farinelli, Kelly Stifter

Members that have left the group during the last grant period:
Research associates: Oleg Kamaev (Queen's University)
Graduate students: Xinjie Qiu (2010 - Stanford University), Matt Fritts (2011 - TU Dresden), Kris Koch (Wells Fargo)
Undergraduate students: David Strandberg, Sean Vigg, Matt Epland, Jeff Gunderson, Chelsea Dorrow
Cryogenic Technician: Roxanne Radpour (supported by SuperCDMS R&D and GEODM)

3.2 Overview

Over the last decade, a variety of cosmological observations, from the primordial abundance of light elements to the study of large-scale structure, and from the observations of high-redshift supernovae to the detailed mapping of the cosmic microwave background, have all led to the construction of a concordance model of cosmology. In this very successful model the universe is made of 4% baryons, 23% nonbaryonic dark matter and 73% dark energy. Understanding the nature of dark matter is one of the leading challenges in particle physics over the next decade, with direct detection of astrophysical WIMPs forming a necessary corollary to the discovery of new particles at the LHC. The unique combination of ionization and athermal phonon signals provided by the CDMS-II ZIP detectors (Z-sensitive Ionization and Phonon) has supplied world-leading WIMP sensitivity for more than a decade. Results from a blind analysis of the last germanium CDMS-II data set, corresponding to 194 kg-days exposure after all cuts, were published in Science [21]. Since that time, we have reanalyzed both the germanium and silicon data using improved pulse-finding algorithms and likelihood methods, pushed our thresholds down to several keV to look for low mass WIMPs [22, 23, 24], completed the analysis of silicon data [25, 26] in which three candidate WIMP events were found, published limits on annual modulation [27], inelastic dark matter [28] and axions [29]. Our recent papers included a refined energy scale determination completed in the last year, as well as

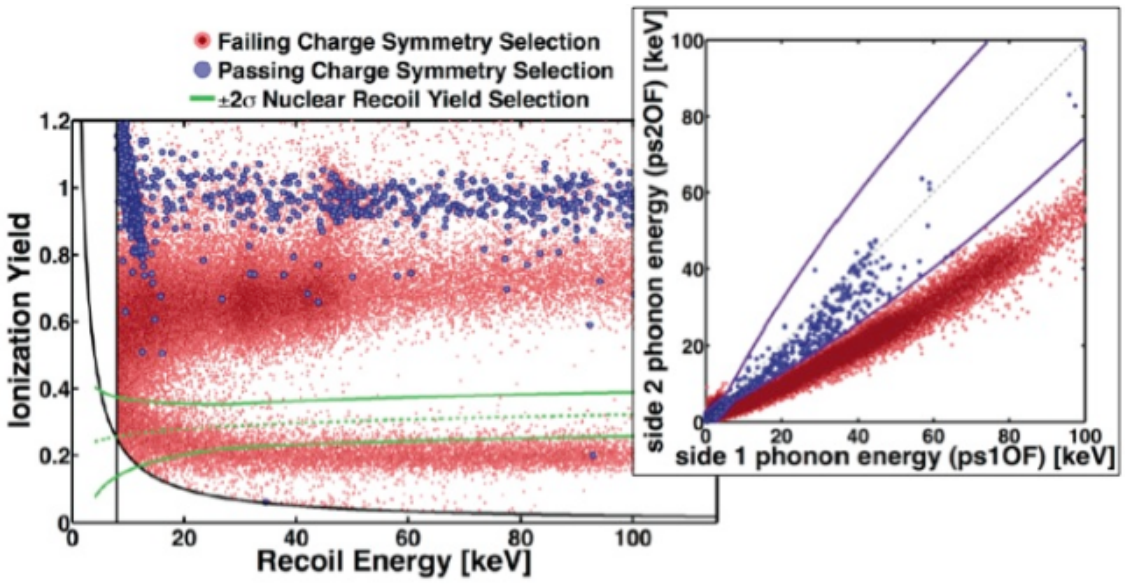

Figure 18: Left: Ionization yield versus phonon recoil energy for nuclear recoils from ^{252}Cf (green, low yield) and bulk electron recoils (blue, high yield) identified as passing the charge symmetry cut. The red surface events are composed of moderate yield electrons from ^{210}Bi and ^{210}Pb beta decay and a low yield band of ^{206}Pb recoils. Right: The same data showing how phonon asymmetry cuts also have discrimination value.

improved neutron background determinations. We published a joint publication with EDELWEISS [30], which improved our high mass spin-independent limit by combining the data sets from both experiments, an exercise we will continue in the future as we strengthen our mutual cooperation in germanium technology.

The SuperCDMS-Soudan experiment was commissioned in the Fall 2011. Five towers, each hosting three iZIP detectors with double-sided phonon sensors and interleaved electrodes are now running. The interleaved electrodes produce an internal field that sweeps both electrons and holes to one side for surface events, while allowing bulk events to deposit energy on both sides. Surface events can then be rejected, since they do not have signals on both sides (charge symmetry cut). The resulting excellent surface event rejection has now been demonstrated underground as shown in Figure 18 and described in [31]. Two detectors were exposed to thin wafers loaded with ^{210}Pb, allowing for a rapid accumulation of surface contamination. The data shown in Figure 18 comes from 900 live hours from one of these detectors and demonstrates surface event rejection efficiency $< 1.7 \times 10^{-5}$ in the 8-115 keV window, while maintaining $\sim 50\%$ efficiency for a 60 GeV/c^2 mass WIMP. In other words, the surface event rejection provided by the iZIP technology renders the surface event background negligible for the SuperCDMS-Soudan experiment, and for the 200-kg SuperCDMS-SNOLAB experiment it would result in < 0.6 background events for 0.3 ton-year exposure. This is conservative, since the estimation is made only using the charge variable. We expect even better surface discrimination in combination with the additional variables of phonon timing and phonon asymmetry. A subset of the lowest threshold germanium iZIP detectors running now will be unblinded by September 2013, providing an independent check of the ~ 8 GeV/c^2 WIMP hinted at by the CDMS-II silicon data, while the standard threshold run including all detectors will run for another 6 months. Depending on the results of the low threshold blind analysis, we may explore installation of silicon iZIPs.

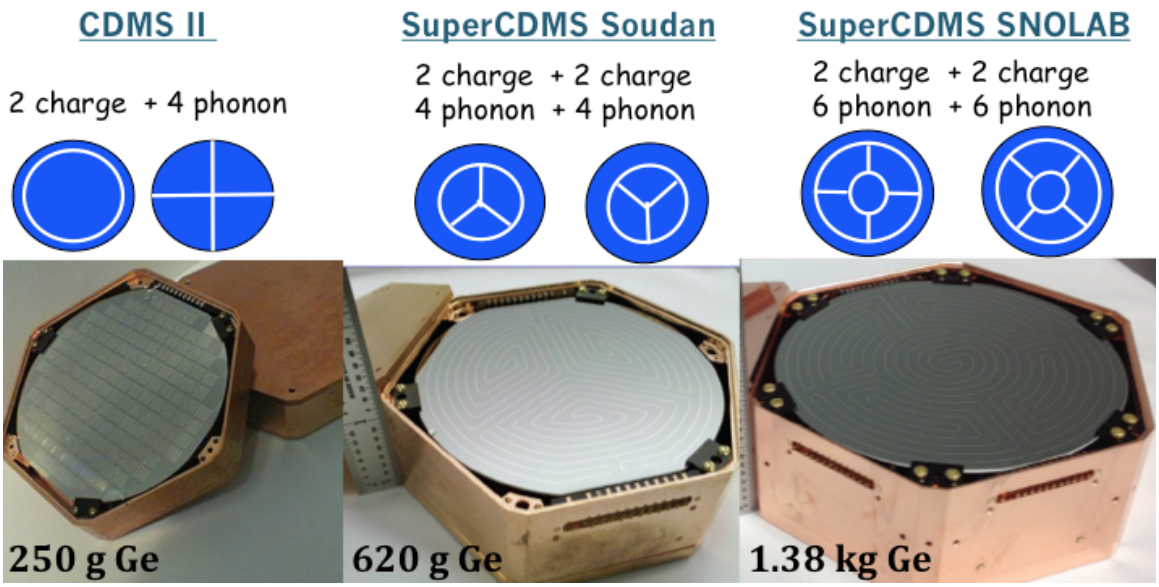

Figure 19: Detector configurations for the three CDMS experiments discussed in this proposal.

Meanwhile, we continue to design our next generation experiment for the deeper SNOLAB site, with the 200 kg germanium detector target. These three stages of our detector development are shown in Figure 19. The new SuperCDMS-SNOLAB 100 mm diameter iZIP detectors are a big step forward in mass, enabling fast and cost-effective construction of the 200 kg payload. Prototype detectors are being tested now in the Minnesota cryogenic lab. Other on-going SNOLAB R&D efforts include designing new cold hardware (from coaxial cable design to FETs to SQUIDs), screening of new shielding and tower materials, shield and neutron veto design, background estimates in the new environment, and a new DAQ.

Our current limits and projections for SuperCDMS at Soudan and then SNOLAB are shown in Figure 20. SuperCDMS-Soudan has the best sensitivity for low mass WIMPs, a region that has become more interesting due to a large number of experimental hints in this region, and that is of particular interest for non-minimal supersymmetric models and for asymmetric dark matter models. SuperCDMS-Soudan also has the most detailed information and best electron recoil rejection in the high mass region preferred by cMSSM theory and by generic WIMP scattering models based on the Higgs boson exchange. These trends will be continued with the SuperCDMS-SNOLAB experiment, which will effectively explore the entire accessible low WIMP mass parameter space, as well as a large fraction of the parameter space at high masses. In particular, the sensitivity of SuperCDMS-SNOLAB at 8-10 GeV will be sufficient to reach the solar (^{8}B) neutrino background, providing a unique calibration signal for this experiment [32].

The Minnesota group has taken the lead on the reanalysis of the corrected CDMS-II data, applying neural network techniques and exploring systematics in much greater depth. This provided theses for grad students Hofer and Zhang under the leadership of postdoc Villano, who is organizing the effort across institutions. Fallows' thesis is also on CDMS-II data, concentrating on the low-threshold analysis, specifically understanding the nuclear recoil energy scale. The new analysis techniques and an improved understanding of both the nuclear and electron recoil spectra at low thresholds are being applied to the new SuperCDMS data.

Minnesota has a robust program of germanium detector characterization and R&D in our cryogenic

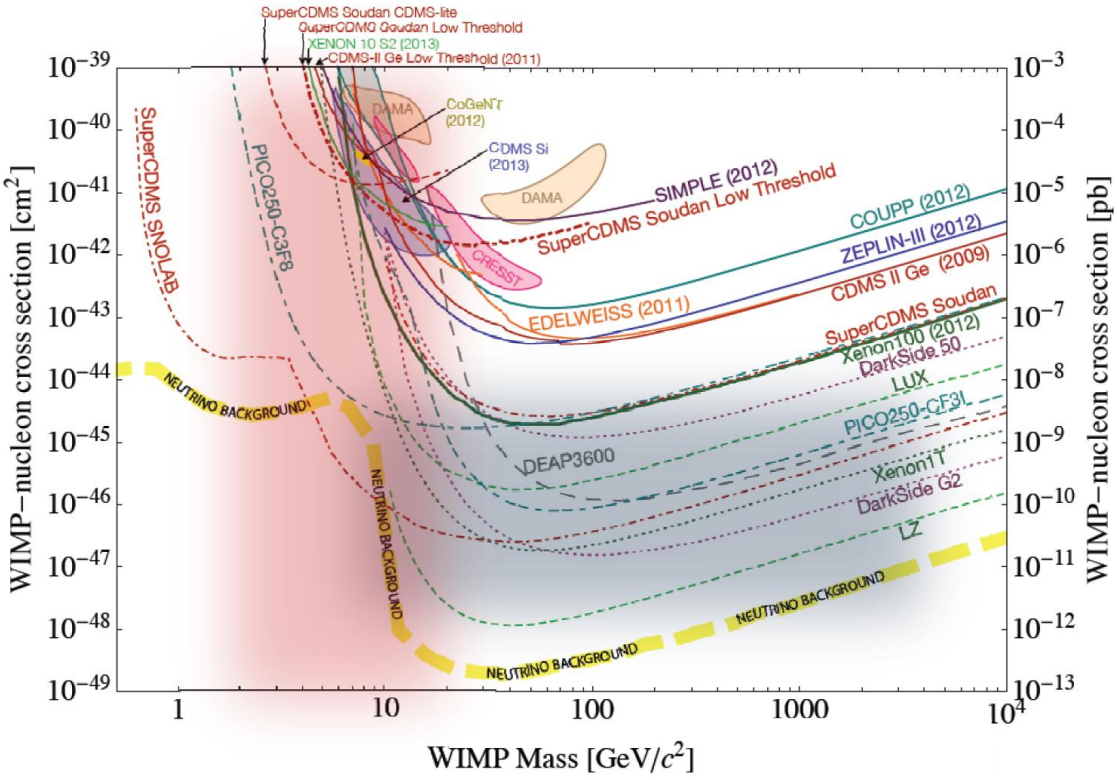

Figure 20: Recent upper limits (90% C.L.) on the WIMP-nucleon spin-independent cross section versus WIMP mass are shown in solid for current experiments, including CDMS II [21]. Dashed and dotted curves denote projected sensitivities of ongoing and future (G2) experiments, including the final SuperCDMS-Soudan sensitivity and SuperCDMS-SNOLAB. These curves are contrasted with the theoretical regions preferred by models of asymmetric dark matter (pink) and constrained MSSM and Higgs-exchange scattering models (grey). Also shown is the limit to WIMP sensitivity induced by the irreducible neutrino background, composed of solar, atmospheric, and diffuse Supernova contributions [32].

lab. The detectors for the currently running SuperCDMS at Soudan have passed through this facility and we are currently the only test facility capable of handling the larger SNOLAB crystals. Postdoc Chagani organizes the characterization runs in the test facility and was aided by technician Radpour. This has the additional benefit of providing cryogenic and hardware experience for all of our students.

The Minnesota group continues to be involved in all aspects of the commissioning, installation, and running of SuperCDMS Soudan and in the design of the new SNOLAB experiment. Besides the running the cryogenic test facility, our responsibilities include upgrading the DAQ and monitoring scripts, taking shifts, screening materials, analyzing the new data, and running simulations to understand the background rates of environmental gammas, and radiogenic and cosmogenic neutrons. Professor Mandic oversees the cryogenic and crystal work, while Professor Cushman concentrates on backgrounds, the SNOLAB neutron veto, and Soudan operations. All members of the group participate in the data analysis which is coordinated between Cushman and Mandic, and the larger

SuperCDMS Analysis team.

3.3 Analysis of CDMS-II and SuperCDMS-Soudan Data

The CDMS-II data set has produced several scientific publications and the data are still actively used for background estimates, to hone new analysis techniques, and to perform new analyses. Minnesota is the lead institution on this legacy data which provided thesis topics for Zhang, Hofer, and Fallows. Newer students trained on this data are now applying new techniques to the SuperCDMS-Soudan data, especially new low threshold data that will be released in just a few months.

3.3.1 Data Reanalysis

In September 2010, the CDMS II collaboration decided to reprocess the data used for the 2009 blind analysis [21] using an improved algorithm for fitting the ionization pulses. Minnesota graduate students Zhang and Hofer played leading roles in the reprocessing of the data (both germanium and silicon), which took place between October 2010 and January 2011. A Reanalysis Working Group was then formed, led by Minnesota postdoc Anthony Villano, with the purpose of doing a blind analysis of the reprocessed germanium and the never-before analyzed silicon data, with Minnesota and Syracuse working on the germanium and MIT on the silicon. Zhang carried out the standard timing cut analysis with a much more extensive set of systematic studies than ever before, while Hofer developed a neural network analysis to optimize separation contours between nuclear recoils and surface events. The advantage of a neural networks approach is that the contours can be arbitrary curves in the 2-dimensional principle component space using the two best linear combinations of four timing variables and trained on the calibration data. A set of cuts was also determined by a 5-dimensional energy-dependent χ^2 analysis (Syracuse) and all three of the independent analyses were cross-checked against each other before unblinding. Since the 5D χ^2 method gave the best sensitivity for higher masses, this was chosen as our official best limit.

Upon unblinding, no events were found in the region of interest with the 5D χ^2 cut, whereas 2 and 3 events respectively were found in the neutral network and standard cuts. Figure 21 (left) shows the corresponding preliminary 90% confidence upper limits, improving by 2× over the original CDMS II result [21] for the standard analysis threshold of 10 GeV. The results of all three analyses were presented by Hofer at the 2013 APS meeting and the paper will be submitted for publication in September 2013. Interestingly enough, when optimized for lower WIMP masses, the neural network approach gives the best limit. In light of the hint of a signal in the silicon data (see below), Hofer is now applying his neural network approach to lower the threshold in the CDMS-II silicon and germanium data. This analysis should be complete by November 2013.

Analysis of silicon reprocessed data has also been completed [25, 26], resulting in 3 observed events with the expected surface-event background of $0.41^{+0.20}_{-0.08}(stat)^{+0.28}_{-0.24}(syst)$ and with the expected neutron background < 0.13. Simulations of this background model indicate 5.4% probability of a statistical fluctuation producing 3 or more events in the signal region. Since these events are distributed at low energy, the profile likelihood ratio test prefers an 8.6 GeV/c^2 WIMP+background hypothesis over the background-only hypothesis at the 99.81% confidence level ($p-$value of 0.19%), giving a WIMP-nucleon cross section of 1.9×10^{-41} cm^2, see Figure 21 (right). Minnesota contributed to this effort in the reprocessing, cuts, efficiency, background estimate, and paper committee.

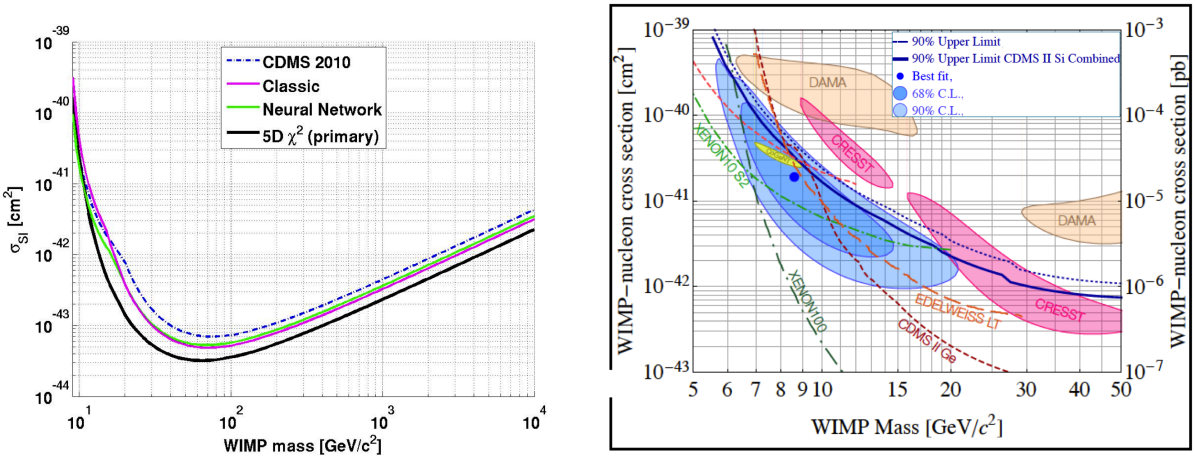

Figure 21: Left: 90% confidence upper limits computed with 3 different analysis methods for reanalysis of CDMS II germanium data. Right: 68% and 90% confidence contours obtained using CDMS II silicon data is compared to limits from CDMS Ge, Edelweiss [41], XENON10 low threshold analysis [42] (revised upward by P. Sorenson), and XENON100 [43]; and to possible signal regions associated with CoGeNT [44], DAMA/LIBRA [37], and CRESST [35] .

3.3.2 Nuclear Recoil Energy Scale

The electron recoil energy spectrum from the ZIP detectors is well-understood, since there are clear gamma lines from both the ^{133}Ba calibration source and from germanium activation after neutron calibration with ^{252}Cf. This does not immediately give us the energy calibration for nuclear recoils, since we need to account for the energy-dependent quenching factor. At low mass, our limit curve is steeply falling, so this uncertainty must be pinned down, even though it is much smaller than the corresponding scintillation efficiency uncertainty in Xenon. Fallows has been part of the 3-person team writing the soon-to-be published energy scale paper, and has done the majority of the work. He minimized the χ^2 between data and Monte Carlo by scaling the phonon energy calibration factor and also compared the energy-dependent quenching factor in our data to a Lindhard [45] parametrization of ionization for well-defined recoil energies, where the parametrization was derived by matching to published results from other experiments. Over the last year, he expanded the analysis to the silicon detectors as well as the rest of the germanium detectors. A resonance in the silicon recoil spectrum allows a more precise determination of the energy scale, and suggests that the recoil energy is underestimated by 10%, which shifts the silicon limit to slightly higher cross sections, see Figure 22. In the 2-30 keV range the germanium recoil spectra were found to be in very good agreement with Monte Carlo, suggesting the published low threshold limits are correct. Fallows presented this (his thesis) work at the April 2013 APS meeting. The nuclear recoil paper should be submitted by the end of 2013.

3.3.3 Ongoing and Future Analyses

Minnesota group is also contributing to the analysis of data acquired by the SuperCDMS-Soudan experiment. Kennedy and Hofer have tackled the critical issue of ionization collection stability of the iZIP detectors, and have defined the criteria for evaluating the detector stability as a function of time. D'Ann Barker, a new CDMS graduate student, studied the chi-squared fits to ionization

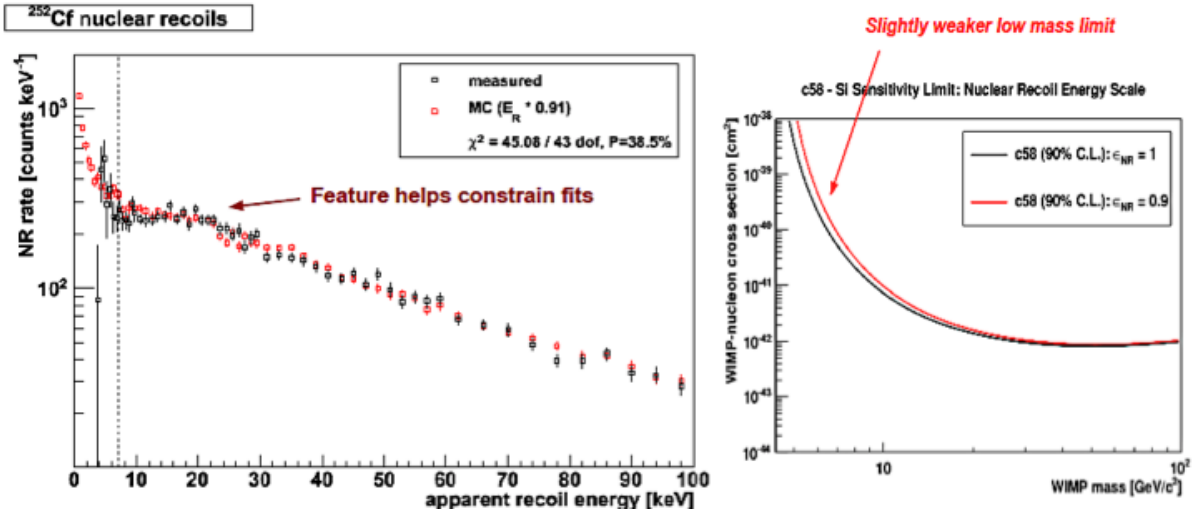

Figure 22: Left: Comparison of Monte Carlo (red) to data (black) showing good understanding of the silicon nuclear recoil scale. Right: effect on low mass WIMP limits of a 10% underestimation (red) in the scale.

pulse shapes to understand times of high noise and other pathologies - all a part of defining the quality cuts required for this new data. All these students are expected to continue their strong involvement in the analysis of SuperCDMS-Soudan data, leading to new measurements of WIMP-nucleon scattering cross section. The Soudan experiment will be completed in 2014, and we expect the analysis of this data to continue through 2015 (years 1 and 2 of this proposal).

We will also initiate a new analysis direction, based on the recent development of the general non-relativistic effective theory for dark matter direct detection [46]. Rather than making assumptions about couplings driven by specific models of the electroweak scale or by appeals to minimalism, this theory considers the most general possible interactions with nucleons. Instead of the traditional spin-independent (SI) and spin-dependent (SD) nuclear responses, the general effective theory includes five: the standard SI response, two types of spin-dependent responses, SD1 and SD2 (longitudinal and transverse relative to the momentum transfer, a particular combination of which is the usual SD), a response which for certain elements is significantly dependent on the angular-momentum of unpaired nucleons (LD), and a novel response which depends on the product of spin and angular momentum (LSD). It has already been demonstrated [47] that interference between operators with similar quantum numbers could significantly alter the strength with which WIMPs couple to a particular target nucleus. Graduate student Kennedy will develop the software infrastructure needed to constrain this multi-dimensional nuclear response space, starting with CDMS II measurements of the nuclear recoil energy spectra in germanium and silicon targets. Once the infrastructure is developed, we will apply it to measurements with other target materials, as well as to the upcoming measurements by SuperCDMS-Soudan. Our goal is to place new constraints on these nuclear response couplings, taking into account possible complementarities between them [47]. This study will deepen our understanding of how experimental results obtained using different target nuclei relate to each other, which is particularly important in light of the recent multiple hints of low-mass WIMP signals.

Since our group will be operating numerous 100 mm iZIP detectors within the SuperCDMS-SNOLAB detector characterization program (see below), we will be at the forefront of develop-

ing the analysis algorithms required to optimally extract information from detectors with a more complicated channel configuration, as well as different noise, charge collection and neutralization properties. The most critical include developing algorithms for determination of event position and surface event rejection, as well as studying the ionization collection efficiency and stability. We discuss these in more detail below, but mention them here to emphasize that new analysis algorithms determined in a test facility will form the basis for analysis of SuperCDMS-SNOLAB data when it becomes available.

3.4 SuperCDMS Soudan DAQ

Minnesota was responsible for the design and operation of the new CDMS-II data acquisition (DAQ) system when the experiment was relocated to Soudan. Reisetter and a previous UM postdoc (L. Duong), developed the overall architecture and wrote the event builder and the online analysis monitoring module. The analysis module gives immediate feedback on parameters like the yield or neutralization; it automatically checks for anomalies, and provides error notification and logging. Details of the DAQ can be found in the recent NIM article [40] written by Cushman. We continue to upgrade the system: Fallows designed and coded the new Soudan data quality monitoring system, which performs real-time analysis on data files as they are created. It gives near-instant feedback to operators on the suitability for low background running of the noise environment, ionization and phonon channel performance of the detectors, triggering behavior, and operation of the veto shield. It interfaces with a database, logging long-term charge and triggering stability information, allowing operators to easily perform web-based analysis of detector properties, checking for performance variations over long time scales. This system is used to monitor the performance of the detectors and the DAQ system in real time, both by the crew at Soudan and remotely by the off-site shift crew. New student Kris Koch has added trending histograms and continues to improve its functionality.

3.5 Backgrounds

Neutron-induced single scatter nuclear recoil events are indistinguishable from WIMPs. The strategy to keep this background to a minimum is to optimize the shielding and to calculate the remaining neutron leakage fraction using a combination of simulation, screening, and data benchmarking. The most dangerous neutrons are those produced by cosmic rays that are not vetoed by the scintillator surrounding the detector and those produced by spontaneous fission, or alpha-n interactions, in the detector assembly and shielding.

3.5.1 Neutron Simulations

Estimating the number of background cosmogenically-produced neutrons requires a Monte Carlo that includes nuclear processes down to low energies in order to generate a neutron energy and angular spectra at the depth of the Soudan mine using the measured muon flux. The Geant4 simulation package has undergone many upgrades to improve the physics needed for underground science. The newest release of Geant 4.9.5 included results of our collaboration with Dennis Wright (of the SLAC Geant4 Collaboration) to improve neutron physics. We have run (and rerun due to bugs in the Geant 4.9.5 release) a high statistics set of the entire SuperCDMS geometry at Soudan, propagating hadronic showers through 10 meters of rock, tracking all produced particles (including neutrons) as they enter the cavern and interact with the shielding and the detectors. The

resulting neutron rates are significantly higher than in previous simulations, but so are the average multiplicities. For the first time ever Geant4 is able to reproduce the absolute nuclear recoil rates in our detectors; we previously normalized our results to the handful of veto-coincident neutrons in the data.

This work is broadly applicable to all underground experiments and our work on the new Geant4 physics lists have been shared worldwide as part of the AARM collaboration (PI Cushman), resulting in much closer agreement between data and Monte Carlo in dark matter experiments running at many different underground labs. Reisetter (as a Minnesota postdoc) was in charge of the CDMS-II simulation. As an adjunct professor here, she has access to the CDMS cluster, meets weekly with our group, and is working with her own undergraduate students from Evansville University, along with Villano, Cushman, and Hofer to redo the cosmogenic background estimates at Soudan. The new results were part of the backgrounds quoted in the 2013 silicon and germanium papers on the CDMS-II Reanalysis. We have been joined by new collaborators postdoc Elias Lopez and graduate student Leyre Esteban from the Multi-Dark group at Madrid University. Lopez has been in residence in Minneapolis for the last 12 months and plans to stay with us for another year, working on background simulations and low threshold analysis. Esteban's visits are for 3-weeks twice a year. She contributes to the veto-coincident data in order to understand muon veto performance and to benchmark the neutron cosmogenic simulations.

Our background from radiogenic neutrons produced in the shielding has been determined by graduate student Mark Pepin in a 2-step process. First, the contamination levels of U/Th/Co/K in the shielding must be determined. Using a Geant4 gamma simulation, each potential contaminant is spread uniformly in the individual shield and structural components and the resulting 35 spectra are added together with scale factors that are allowed to float in a global χ^2 minimization fit to the gamma spectrum observed in our ZIP data, where individual lines can be seen. (see Figure 23). Once contamination degree and type are determined, the neutron-producing spontaneous fission and alpha-n reactions are simulated, weighted by the factors determined by the global gamma Monte Carlo. Resulting rates of single nuclear recoils are convolved with the analysis total efficiency curves to produce the neutron background rates and spectra used in the recent CDMS-II papers on silicon and germanium. The same method is now in process for the SuperCDMS-Soudan data, with summer student D'Ann Barker and Elias Lopez joining Pepin.

3.5.2 SNOLAB Neutron Veto

Using many of the same tools, Pepin has also studied the rates expected at SNOLAB for several passive shielding designs (his neutron rates were used for the SNOLAB R&D proposal). While acceptable for the 200 kg SNOLAB run, the neutron rates assume that screening of samples will be sufficient to establish the required radiopurity levels. If an efficient active neutron veto could be designed, this in-situ monitoring of radiogenic neutrons would ameliorate the risk of incomplete sample screening. Cushman, Chagani and Pepin are studying the design of a gadolinium-loaded scintillator surrounding the cryostat in collaboration with FNAL. Much of this work will be design optimization using the Geant4 Monte Carlo, but this can only go so far without an estimation of the achievable light yield and neutron capture efficiency of scintillator we can actually produce, as well as the photodetection properties and noise thresholds encountered when reading out real scintillator samples using wavelength shifting fibers and silicon photomultipliers (SiPM). Thus, a scintillator testing program has been initiated. While FNAL is pursuing a liquid scintillator option, Minnesota is proposing a design using solid Gd-loaded block polymers to increase the neutron

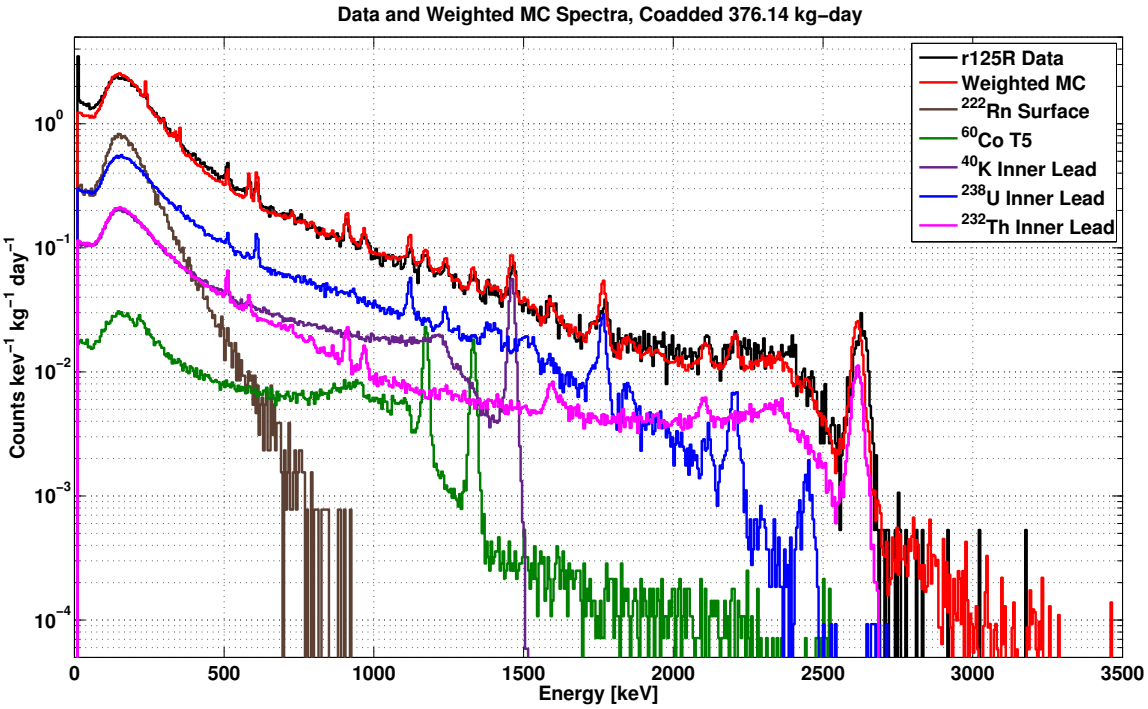

Figure 23: A global gamma simulation (red) is fit to the CDMS-II detector electron recoil spectrum (black) to determine the level of contaminants in the Soudan shielding and tower materials. Several examples of the individual spectra used in the fit (per contaminant and per shielding element) are also shown.

capture efficiency.

Solid scintillator has some advantages over liquid: lower cost, no containment vessel or purification plant, and modular construction without risk of leaks. However, light yield in plastic scintillator tends to be compromised by increased concentrations of the neutron capture material. We plan to explore new ways to incorporate fluors with gadolinium, lithium, and boron additives in PVT, PMMA and polystyrene matrices using several methods of polymer catalysis, ligand chemistry, copolymerization, and epoxy techniques. The Polymer Chemistry Group at the University of Minnesota is composed of members from the departments of CEMS (Chemical Engineering and Material Science) and Chemistry. Professors Marc Hillmyer and Frank Bates are world experts in polymer chemistry and are collaborating with us on creating a novel neutron-sensitive plastic scintillator which would be generally useful for nuclear physics and homeland security. Their students make scintillator samples for us with chemicals that we purchase, using the chemistry lab infrastructure. The samples are thermally polymerized in glass ampules, which are then broken to extract the solid samples. The entire process will be supervised by Cushman and Chagani, with frequent input from Bates and Hillmyer, as they suggest possible avenues to improve the characteristics.

Over this summer the chemistry department has already produced solid scintillator samples following the scintillator cocktail described in Ovechkina et al. [49]. The samples were sliced, grooved, and equipped with a WLS fiber center at the physics shop. In our optics lab, four new SiPMs were acquired and a low noise readout system installed. Standard photomultiplier tubes are not sufficiently radiopure for this application. The SiPMs were used to read out the scintillator samples, as shown in figure 24 where photoelectron peaks up to ~ 7 pe can be clearly identified. The optics lab

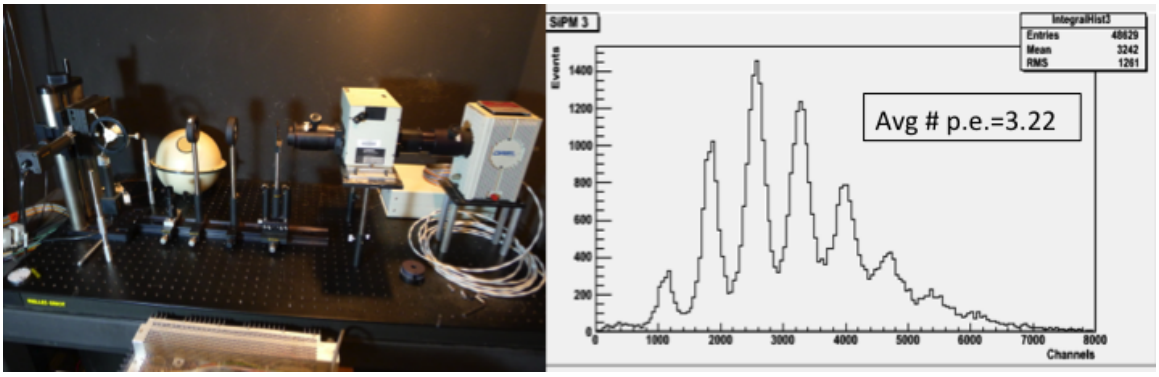

Figure 24: Solid scintillator samples (far left of dark room photo) made at the University of Minnesota (polystyrene with POPOP and PPO), activated with a blue led and read out by WLS fibers and four different SiPMs (Russian CPTA 143-30; MRS APD), demonstrating the excellent photon counting properties achieved in our lab.

was originally equipped by Cushman to develop the readout for the CMS Hadronic Calorimeter, and eventual quality assurance for 10,000 hybrid photodiode channels. We will use it to measure absolute light yield, neutron efficiency, quantum efficiency, gain, and spectral response, as well as attenuation and uniformity (using the nanomover). A cooling system to stabilize the gain (and noise) of the SiPMs is under construction. This optics lab will be used to characterize the optical properties for both solid and liquid prototypes, as well as develop the SiPM readout for whichever option is finally chosen.

3.5.3 Radiopurity Screening

In order to improve our contaminant estimates, a high-purity P-type coaxial germanium detector (HPGe) was installed in the Soudan mine in February 2008, and was then equipped with a higher purity copper-lined lead shield using DOE ARRA funds. This reduced the background by a factor of 20 overall and we are now achieving U/Th sensitivity levels of $<$1 mBq/kg for a standard 2-week run and $\sim$ 0.2 mBq/kg for selected 40-day runs. Other ARRA improvements include a new radon purge unit with sample load-lock, which reduces radon inclusion wait times from 3 days to 6 hours, improving the livetime. A new computer-controlled LN auto fill provides hands-free maintenance.

Undergraduates have helped with all aspects of this project, from installing the detector, to building the shielding, to measuring U/Th content in samples. Summer students helped develop an automated script, which streamlines peak finding and contaminant estimation. We no longer use the Genie software that came with the Canberra HPGe DAQ, since we have moved to a more sophisticated, in-house simulation program to treat background from the shield and to calculate the absorption efficiency from any shape sample. We have run samples of shield material, as well as possible materials (carbon fiber, titanium, zirconium oxide) for SNOLAB tower support and infrastructure. The HPGe will be in continuous use over the next two years and is our main tool for understanding bulk contamination. Soudan staff changes samples, but Pepin does the analysis of each sample and maintains the screening spreadsheet. The results also need to be checked for U/Th secular equilibrium and scanned for other anthropogenic and neutron-activated contaminants.

3.6 CDMS Cryogenic Laboratory

Our cryogenic laboratory operates two cryostats, known as Little Blue and K100. During the last grant period, we have made advances on a wide variety of instrumental efforts using these two cryostats, ranging from the SuperCDMS-Soudan detector testing to R&D work for SuperCDMS-SNOLAB.

3.6.1 Cryogenic Facility and Detector Testing for SuperCDMS-Soudan

Little Blue is a Janis CF-25 helium dilution cryostat characterized by short turn-around time. It is ideal for performing critical functionality tests of new detectors, such as measurements of the critical temperatures and currents of phonon channels. These measurements provide important fast feedback to the detector fabrication teams at SLAC, Stanford University, and TAMU, directing the subsequent optimization of the detector fabrication. Six 75 mm diameter Ge iZIP detectors were characterized in this cryostat, two of which needed minor repairs before being deployed in the SuperCDMS-Soudan experiment. We also developed a new wiring scheme that allowed us to perform critical temperature measurements of up to 20 samples in a single run. This feature was used to provide fast feedback to our collaborators at TAMU, who were developing a new detector fabrication facility needed for the 200 kg and 1 ton scale germanium dark matter experiments. We measured 50 small samples, two thin test wafers, and the first full 75 mm iZIP detector fabricated at TAMU. Results of these measurements have guided the TAMU team in tuning their fabrication process, allowing them to quickly bring their facility online. The Little Blue team was headed by M. Fritts until his departure in 2011, and more recently by A. Villano. Graduate students T. Hofer and A. Kennedy were also heavily involved.

K100 is a Kelvinox-100 dilution cryostat, characterized by 100 μW cooling power and a relatively large detector volume, capable of hosting up to 150 mm diameter germanium or silicon crystals and all of the standard CDMS readout hardware. The cryostat can support up to four Detector Control and Readout Cards (DCRCs), developed by our FNAL collaborators to bias, read out, and digitize the ionization and phonon sensors. The pulse data acquired by DCRCs are analyzed with the standard CDMS data analysis pipeline operated on a local computing cluster, providing near real-time analysis of the acquired data. Over the last grant period, we have complemented the cryostat with a new leak detector (using Mandic's McKnight fellowship funds), and we constructed a lead and polyethylene shield around the cryostat to suppress the ambient gamma and neutron background by 5-10$\times$ (designed and built by graduate and undergraduate students). We measured the performance of the shield, as well as the ambient background in the laboratory using a high purity Ge gamma spectrometer, borrowed from the department. We have also acquired a number of gamma, beta, and neutron sources that can be used to study detector response to different types of interactions in the crystal. K100 is now a very versatile facility, capable of conducting all detector characterization measurements from basic functionality tests to the most detailed detector performance characterization, such as measurements of the neutralization hold-time or surface event rejection efficiency.

Several of the K100 runs were devoted to the new DCRC electronics. While many DCRC tests can be performed on the bench, the ultimate performance characterization (such as noise level measurements) could only be performed with real detectors. We hosted several visits from our FNAL colleagues who designed the cards, and with them we conducted a series of measurements providing feedback on the DCRC design. This work resulted in several upgrades to the DCRC,

ultimately leading to the new version of the card with excellent noise performance. In addition, these runs enabled optimization of the data acquisition software used to operate the DCRCs. For example, our facility was the first to synchronously operate three DCRCs, which was necessary to operate 100 mm iZIP detectors.

Several of the K100 runs were devoted to the SuperCDMS detector characterization program. Six 75 mm diameter iZIP detectors (G41, G42, G19N, G16K, G53, G51) were characterized in detail prior to detector installation at the Soudan mine in October 2011. We established the neutralization hold-time for these detectors, and we assessed the performance of their phonon and ionization channels. These measurements were critical in deciding whether the detectors can be operated in the dark matter search at Soudan, and they informed the optimal scheme for operating the detectors at Soudan. We also operated G21A, a 75 mm crystal with iZIP phonon sensors deposited on a single side, which was the first 1cm thick device fabricated at TAMU. First phonon pulses were observed with this device, thereby reaching a milestone for the new fabrication facility at TAMU. The K100 team is overseen by Mandic, and includes postdoc H. Chagani and graduate students Zhang, Kennedy, and Radpour.

3.6.2 R&D of 100 mm iZIP Detectors

Following the installation of the SuperCDMS-Soudan experiment in October 2011, the focus of K100 operations shifted to the R&D of 100 mm diameter germanium detectors, which are being developed for the SuperCDMS-SNOLAB project. The SNOLAB experiment includes 200 kg detector target mass, so increasing the size of individual detectors is critical in order to keep detector fabrication and testing costs low, to reduce the amount of wiring and heat load on the cryostat, and to simplify the installation.

For the past two years K100 has been the only cryostat in the SuperCDMS collaboration capable of operating 100 mm detectors, which placed our group on the critical path of this R&D effort. Since 100 mm crystals were never operated at $\sim$ 50 mK, our first objective was to establish that they can support high ionization collection efficiency. While these crystals are of the same type as the standard 75 mm detectors, the density of dislocations in the crystal is known to grow with the radial position—dislocations act as charge traps and could therefore compromise ionization collection. We started with ionization-only 100 mm diameter, 34 mm thick germanium devices (G101a, G102a), with four concentric electrodes deposited on one side of the crystal (and the opposite side grounded). We used slightly modified hardware for CDMS detector readout (shown in Figure 25 (left)) with two synchronously operated DCRCs. Several runs were conducted with these devices, placing ^{241}Am (60 keV) gamma sources in different configurations to expose both sides of the crystal at different radial positions. Data acquired in these runs allowed us to study the performance of the crystal on both surfaces, to measure charge collection efficiency as a function of radial position, and to study the propagation of electron and hole charges through the bulk of the crystal. Another ionization-only device (G101b) with a two-electrode design similar to that of 100 mm iZIPs was also successfully tested.

Figure 25 (middle) shows an example of the ionization spectra obtained with four-electrode device G102a, with clearly resolved 60-keV peaks due to ^{241}Am sources. Positions of the 60-keV peaks were measured for each of the three inner electrodes as a function of the bias voltage. We found that the ionization collection efficiency approaches 100% when the voltage bias across the crystal exceeds $\sim$ 3 V (see Figure 25 (right)), which is consistent with the past measurements performed using smaller crystals. Similar measurements were made at higher energies (356 keV) using an external

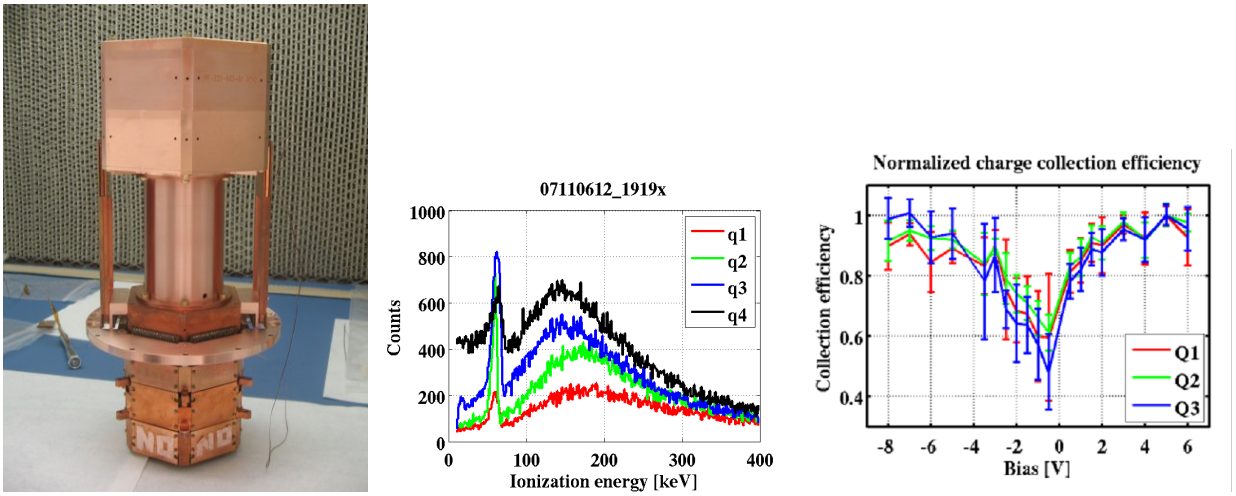

Figure 25: Left: Installation of a 100mm diameter crystal with the standard 75 mm CDMS readout hardware. Middle: Ionization energy spectra measured with G102a with four different electrodes. The 60-keV gamma peaks due to the ^{241}Am sources are clearly identified in the spectra. Right: Ionization collection efficiency as a function of bias voltage across the G102a crystal, measured using the positions of ^{241}Am 60-keV peaks.

^{133}Ba gamma source. The neutralization hold-time for all of these devices was over 20 min, after which the crystal could be neutralized with the standard techniques using infrared light exposure. Similar hold-times were observed for the past smaller crystals. These studies were published in [48] (with H. Chagani as the lead author) and were presented in multiple international conferences as a demonstration that 100 mm diameter, 34 mm thick germanium crystals can be used to build CDMS-style dark matter detectors.

More recently, first full 100 mm iZIP detectors were fabricated by our collaborators at SLAC (G103a, G106a). Unlike the 75 mm detectors, these detectors have 6 phonon channels on each side and 2 ionization electrodes on each side. Consequently, they require 3 sets of the standard electronics, including 3 SQUETs (housing SQUIDs and FETs for the first stage amplification of phonon and ionization signals respectively), and 3 DCRCs operated synchronously. We assembled the necessary hardware and operated these iZIPs in the K100 cryostat. We performed detailed characterization of all channels of these detectors, including the critical temperature and current, noise levels, optimal bias levels, neutralization hold time, and breakdown voltage. Both crystals performed very well, and with the exception of one channel, all channels met the specifications for a dark matter detector. Detectors were exposed to a single ^{241}Am source collimated above one of the phonon channels, and data was acquired using different ionization bias voltages and optimal phonon bias voltages. The analysis of this data is in progress, and although hampered by the misbehaving channel, some interesting results were obtained, such as the recovery of the position of the ^{241}Am source. Postdoc Chagani organized this work and led most of the runs, under Mandic's supervision and assisted by technician Radpour, graduate students Kennedy and Zhang, and undergraduates Strandberg, Codoreanu, and Phenicie.

3.6.3 Cold Hardware Design

The design of the CDMS II ionization readout chain (inside the cryostat) was driven by the need to minimize the coupling of microphonic noise into the gate (JFET) wire of the charge amplifier, while keeping the capacitance to ground at a minimum. This led to the use of rigid vacuum coaxial cables, and in turn to the current mechanical design (see Figure 25 left). Along with collaborators at SLAC, we started to explore whether there are alternative wiring schemes that could simplify the hardware design of the resulting electronics tower. A flexible TexCal coaxial cable (copper conductors with graphite-based insulator) was found to have a very similar performance both in terms of background noise levels and in terms of susceptibility to microphonics. We have also explored solutions based on superconducting Nb wires sandwiched between layers of kapton and copper tape, but these options had higher microphonics susceptibility. The project was first pursued by Strandberg (completed his undergraduate senior thesis), and currently by undergrads Codoreanu and Phenicie.

3.6.4 Proposed Research Activities

Our cryogenic lab will play several roles of critical importance to the SuperCDMS-SNOLAB project. In the first year, the focus will be on the R&D of 100 mm iZIP detectors and of the accompanying hardware and electronics. As noted above, 100 mm iZIP detectors have so far been operated using (three sets of) CDMS II 75-mm hardware and electronics. During the first year of this proposal, the design of the 100 mm SNOLAB detectors is expected to be finalized, and the first 100 mm cold hardware and room-temperature electronics (DCRC) prototypes (designed to match the new detectors) are expected to be built. Furthermore, new MIDAS-based data acquisition software is under development and is also expected to become available on this time-scale. In our cryo lab we will test these different components of the experiment: we will characterize detector performance, quantify the noise and mechanical performance of the new cold hardware and of the new DCRCs, and provide the necessary feedback for optimization of these components. We will also operate the new data acquisition software and contribute to its development and troubleshooting. We particularly emphasize the integration aspect of these efforts: our facility will enable bringing these different components together and integrating them into a well-functioning system, well before the experiment begins operations at SNOLAB in 2016. These efforts will therefore be critical for smooth commissioning of the SuperCDMS-SNOLAB experiment.

In the years 2 and 3 of this proposal we expect to be in the detector and hardware production phase of the SuperCDMS-SNOLAB project. All of the detectors and towers will be produced at this time, and our cryogenic laboratory will be an integral part of the project's detector testing and characterization program. While the detailed plans for this program are still being developed, the current scheme includes testing sample detectors from each production batch as well as testing each of the fully assembled towers of detectors. The Minnesota cryo lab will be one of the two lead facilities carrying this testing load (the other being at UC Berkeley). As discussed above, these tests include measurements of the neutralization stability and hold time, ionization collection efficiency, critical temperatures and currents of phonon channels etc. In addition, we will pursue several in-depth studies of the detector performance, resulting in new data analysis algorithms for optimal use of the rich information provided by 100mm iZIP detectors, and potentially leading to detector design improvements. We discuss these further now.

Position Reconstruction: Position reconstruction on an event-by-event basis allows us to correct detector response variations across the detector surface. In CDMS-II, position correction of

the phonon amplitude and timing led to significant improvements in both energy resolution and the timing-based parameters used to identify (and thus reject) surface events. The 100 mm iZIP detectors have a very different phonon sensor configuration, with 6 sensors on each side. New algorithms are therefore needed to reconstruct event position in these detectors. We will expose the 100 mm iZIP detectors to different configurations of multiple collimated ^{241}Am sources. These data will then be used to optimize position reconstruction algorithms and to study their performance for different source configurations. We emphasize that the flexibility of our K100 setup makes these studies possible - these studies cannot be pursued in the large SNOLAB cryostat, where they would impose significant costs in terms of WIMP exposure.

Surface Event Identification: The 75 mm iZIPs operated in the SuperCDMS-Soudan experiment have demonstrated surface event rejection of $< 1.7 \times 10^{-5}$ using the asymmetry of ionization signals on the two detector sides [31]. It is important to verify that the 100 mm iZIP detectors can achieve similar performance. Since 100 mm detectors will not be operated underground soon, we will attempt this measurement in the K100 cryostat. Being near the surface, the ambient neutron background limits our ability to measure the leakage of surface events from the electron recoil band into the nuclear recoil band. To reduce this background, we have built an 8"-thick polyethylene shield around the cryostat, which suppresses the ambient neutron background by 5-10×. A new ^{210}Pb source of low energy betas has already been operated inside our cryostat. Our study of surface rejection will include ionization asymmetry, phonon signal asymmetry, and phonon timing, starting with the prototype 100mm iZIP detectors we have in hand.

Nuclear Recoil Energy Calibration: We will perform nuclear recoil energy calibration of Ge detectors, using our recently-purchased ^{88}Y-Be monoenergetic neutron source (35 keV). We are currently conducting simulations in order to identify the optimal source-detector configuration for this measurement. This measurement is of interest to all germanium-based experiments, especially at low recoil energies where there is disagreement in the literature and divergence from Lindhard theory. Differences in the nuclear recoil scale can move the limit curves for low mass WIMPs by as much as 10%. We will also map out how the nuclear recoil scale changes with bias voltage, since running with much higher bias (CDMSLite mode) will enable us to lower our energy thresholds to tens of eV at SNOLAB (170 eV has been demonstrated at Soudan) to cover the very low mass WIMP region.

Ionization Readout Wiring: The copper-based TexCal coaxial wire may be a good alternative to the vacuum coax design in terms of microphonics susceptibility, but its high thermal conductivity makes it impractical for carrying signals across different temperature stages. Our previous attempts with superconducting Nb wire used standard conductor-insulator interface, and resulted in too high microphonic susceptibility. We propose another alternative, where the Nb wire is painted with a graphite-based paint, sandwiched between two layers of kapton tape, and two layers of Nb tape. This arrangement provides a coaxial cable with the inner (super)conductor separated from the insulator (kapton) with partial conductor (graphite), which may be sufficient to reduce the triboelectric effect in the Nb wire due to microphonics. If successful, this solution could be used to carry signals from 50 mK to 4 K, thereby making the rigid mechanical structure of the Tower unnecessary.

4 Physics at the Intensity Frontier

4.1 Personnel

Faculty: Professor Dan Cronin-Hennessy (25% effort)
Faculty: Professor Ron Poling (75% effort)
Senior Research Associates: Postdoc
Research Associates: Jianming Bian
Research Associates: Hajime Muramatsu
Graduate student: Derrick Toth
Graduate Student: Andy Julin
Undergraduates: Nick Smith

Members that have left the group during the last grant period:
Undergraduate students: Zebulon Perrin

4.2 Introduction

The BESIII experiment at the BEPCII electron-positron storage ring in Beijing, China is currently the world's only accelerator facility operating in the tau-charm threshold region. It provides data samples for the study of open- and hidden-charm particle production and decay that are smaller than those of competing experiments (Belle, BaBar, LHCb, etc.), but are unrivaled in their cleanliness and suitability for precision measurements. BESIII event samples now far exceed those of previous electron-positron collider experiments working in the charm region, most notably notably CLEO-c, from which our group and others from Carnegie-Mellon University, Indiana University and the University of Rochester transitioned in 2008. Table 1 summarizes the data collected by BESIII so far and for the run in progress. The collaboration has used these data to produce many

Table 1: BESIII data samples through March 2013

Data Type	Sample Size	Note
J/ψ	1.2 billion events	20× previous (BESII)
$\psi(2S)$	0.5 billion events	20× previous (CLEO-c)
$\psi(3770)$	2.9/fb	3.5× previous (CLEO-c))
$\psi(4040)$	0.4/fb	$\gg$ previous (CLEO-c)
$Y(4260)$	1.0/fb so far	$\gg$ previous (CLEO-c)
$Y(4360)$	0.5/fb	First data
Misc.		R measurements, τ scan, XYZ scans

interesting physics results, with a total of 43 papers published or accepted based on BESIII data. There have been many talks at international conferences including those by Bian ("A Review of $h_c(^1P_1)$, $\eta_c(1S)$ and $\eta_c(2S)$" at Charm 2012 in Honolulu) and by Poling ("D^+ Leptonic and D^0 Semileptonic Decays: First Results from BESIII" at ICHEP 2012 in Melbourne). The highlight of BESIII physics so far is the recent announcement of the discovery of $Z_c^{\pm}(3900)$, a new charged charmonium-like state observed in $e^+e^- \to \pi^+\pi^- J/\psi$ at $E_{CM} = 4260$ MeV [51].

The Minnesota group joined BESIII with a primary focus on open-charm physics. Tools were adapted from CLEO-c for D-meson tagging that have been used by many BESIII groups. Progress toward open-charm results has been slow, however, because this is precision physics with data samples that are mostly only a few times larger than CLEO-c's. There are many systematic effects and it has been a long road bringing BESIII performance to a level comparable to CLEO-c, especially in tracking. Many improvements have been made and preliminary results have been presented on semileptonic and leptonic D decays. The first Minnesota open-charm study has focused on $D\bar{D}$ production and hadronic cross sections with the goal of resolving an apparent inconsistency between BESII and CLEO-c measurements of non-$D\bar{D}$ decays of $\psi(3770)$. This is the thesis project of Derrick Toth and involves most members of our group. We expect to have results by summer, as is described in Sect. 4.5. Because of the slow progress and need for additional data to complete the non-$D\bar{D}$ measurement, we have also become involved in other BESIII physics projects, including studies of charmonium decay and the very topical investigations of "XYZ" states in data at $E_{CM} = 4260$ MeV and 4360 MeV.

The Minnesota BESIII group is small, and the faculty leading it also have commitments to the long-baseline neutrino experiment NOvA (25% NOvA effort for Poling and 75% for Cronin-Hennessy). Both have had roles in the design of the PVC-module production procedures and in preparations for electron-appearance measurements. With the onset of NOvA data taking later in 2013 (cosmic-ray running is already in progress), Cronin-Hennessy plans to withdraw from BESIII and concentrate all of his research effort on NOvA no later than summer of 2014. Poling will continue his 75%/25% split between the two experiments.

Our BESIII group contributes to the experiment in many ways and we have leveraged support from the University of Minnesota to maintain an effort that is larger than our DOE funding could sustain. In addition to our exceptionally productive postdoc Jianming Bian (also 50% on NOvA), in May we are adding a second postdoc, Hajime Muramatsu, who will be 100% on BESIII for six months and then transition to a 50/50 split between BESIII and NOvA. We continue to hold leadership roles in the collaboration. Poling serves on the collaborations Executive Board, Institutional Board, and Publications Committee. Cronin-Hennessy chairs an important committee evaluating analysis tools for D physics. Both also serve or have served on numerous analysis committees. Bian serves on analysis committees and carries important service responsibilities for the experiment. New postdoc Muramatsu, who is moving to Minnesota from the Rochester BESIII group, is the co-convener of the BESIII charm group and also chairs a number of analysis committees. The junior members of our group are also engaged in BESIII analysis and service. These include grad students Derrick Toth, who supports Monte Carlo production and its analysis infrastructure, and Andy Julin, who has worked on Monte Carlo truth-tagging, tracking-efficiency studies and evaluations of D-tagging tools. Undergrad Nick Smith is working on BESIII analysis and Zeb Perrin was until recently the principal operator of our computer farm and local BESIII librarian. Our computer operation relies on strong support from the School of Physics and Astronomy IT staff, especially Nick Bertrand, who has been partially supported by our BESIII group (university funds) to work on farm management-software upgrades, storage management and networking improvements.

The remainder of this section is organized as follows. Section 4.3 describes the current status of the BEPCII accelerator and BESIII experiment; Sect. 4.4 recounts Minnesota group resources and contributions to BESIII; Sect. 4.5 describes current Minnesota group BESIII analysis projects; and Sect. 4.6 describes completed analyses and other analysis activities.

4.3 BESIII Status

BESIII data collection so far during 2013 has been at $E_{CM} = 4260$ MeV, 4360 MeV and nearby energies. Performance of both the accelerator complex and the BESIII detector have been very good, especially compared to the struggles of 2012. The machine ramped up to good luminosity quickly, achieving a peak luminosity of $\sim 6 \times 10^{32}$ cm^{-2}s^{-1} in 60-bunch operation with 600 mA $\times$ 600 mA currents and maintaining it for the 4260 and 4360 running. BESIII records were set for the best day's and best week's integrated luminosity, 27/pb and 148/pb, respectively. All BESIII subsystems worked well and a new storage ring lattice was implemented successfully. Some noise problems were experienced, both recurrences of old problems and one new one. Nevertheless, the data quality has been excellent.

The successful run at 4360 MeV and brief operation as high as 4416 MeV represent the highest-energy operation so far of BEPCII. This performance has provided encouragement that higher energy reach for R scans and even $\Lambda_c\bar{\Lambda}_c$ data (~ 4600 MeV) may be achievable. Additional running at $\psi(3770)$ and for D_s physics are also in the longer-term plan. For these BEPCII and BESIII will need peak performance. Some challenges remain for the accelerator, notably increasing the beam lifetime and controlling particle backgrounds and accelerator-induced noise in BESIII. The effort to reach design luminosity (10^{33}) will resume at the end of the current run with further efforts to develop improved lattices. BESIII is exploring options for replacing or upgrading the inner part of the tracking chamber, which is gradually degrading due to the background particle flux.

4.4 BESIII Resources and Service

The Minnesota group operates the largest dedicated computing facility for BESIII outside of the host laboratory IHEP. The core configuration remains unchanged since last year, with 50 dual-quad worker nodes each with 24 GB of memory. During the past year we have augmented our data storage facilities both for capacity and for performance. Our main storage has been an Apache Hadoop implementation. Each worker node serves as a data node for Hadoop, and is fitted with three 2- or 3-TB drives. The 300 TB is configured with 3-fold replication and provides a net capacity of 90 TB. In the past year we have added a new RAID configuration based on a FreeBSD ZFS file system. It uses Supermicro 45-drive chassis units populated with commodity 3-TB drives and delivers RAID storage at \$102/TB. The current capacity of this system is 85 TB with the potential to triple as needed. Our experience with this system has been excellent, both in performance and reliability.

The current Minnesota farm produces BESIII simulated events at a rate of approximately 20-25 million per day, including end effects. For each new BOSS version we produce very large event samples for all of the analyses being carried out by Minnesota personnel and also special simulated samples for the collaboration. Networking to China remains sufficiently problematic that large-scale transfers between Minnesota and IHEP are prohibitively time-consuming. For that reason we host only selected samples of data at Minnesota, doing most data analysis at IHEP. We have almost all of our Monte Carlo at Minnesota, however, so design studies, efficiency determinations and systematics studies are done on our facility.

During the past year it became clear that we were far from saturating the Minnesota BESIII farm system, so we have made two adjustments in its operation. First, we became fully integrated into the fledgling BESIII grid computing infrastructure, an effort that is led by personnel at IHEP and UCAS (University of the Chinese Academy of Sciences). At present Minnesota is a Tier 1 site and

the largest remote member of the BESIII grid, in terms of both capacity and production. Although the BESIII grid is not yet available to general users, it is being used routinely by a subset of the collaboration. Derrick Toth is the coordinator of Minnesota BESIII grid participation.

Our second operational adjustment is to make available idle cycles on the BESIII farm to the other research activity for several members of our group, NOvA. This has worked extremely well as NOvA had approached initial far-detector data taking, and with beam coming later this year. Based on this success Poling has obtained additional University resources to add more CPU and storage capacity specifically for NOvA. In the new configuration being assembled at present, there will be equal-sized BESIII and NOvA farms. The jobs of each group will get preference on their respective farms, but jobs will be allowed to expand into the full 800-core facility when the other experiment's processors are idle. To allow for smooth and efficient operation in this cooperative mode, we are updating some aspects of the BESIII farm infrastructure, including returning to CONDOR for job management in place of the current SGE (Sun Grid Engine), which is less prevalent in HEP and faces licensing uncertainties as Oracle manages assets inherited from Sun.

Because the Minnesota group does not have any personnel in residence at IHEP in Beijing, our service tasks for BESIII relate to our computer facility and other remote jobs. For example, Bian has worked on the data-transfer problems between Minnesota and IHEP, establishing and testing bbftp as a transfer tool. He has performed cross-checks of luminosity measurements between different data samples and made an independent luminosity determination for the BESIII tau-scan data. He has also carried out data-quality checks for both tau-scan and the $E_{CM} = 3650$ MeV data sample. Toth has managed the implementation of new EventNavigator Monte Carlo truth-tagging, running jobs at IHEP to reconstruct the raw data files to produce new compressed "dst" files that have Event-Navigator information.

Andy Julin has developed tracking and particle-ID efficiency measurements primarily for D-decay analyses, with a focus on kaons. This project was started to cross-check IHEP studies and to provide us with the tools for systematic studies for our non-$D\bar{D}$ and other analyses. Within a data or Monte Carlo sample Andy selects events with various D^- tag modes and at least two other pion tracks of the correct charge, as would be expected for the "golden" $D^+ \to K^-\pi^+\pi^+$ decay. He calculates the missing four-momentum in the event, accumulates distributions of missing-mass-squared, and fits this to the expected shapes of a kaon signal (with appropriate smearing) and background. By separating the subsamples in which the kaon track is either found or not found by some set of selection criteria, he can directly determine the inefficiency. Extensive Monte Carlo studies were used to develop and test the procedure, which requires reliable determination of true particle identities. Andy developed new tools based on raw-hit tagging to improve the Monte Carlo matching compared to the angular matching that was previously used. Fig. 26 shows example missing-mass-squared fits for one momentum bin and the the data/Monte Carlo comparison for the full momentum range in $D^+ \to K^-\pi^+\pi^+$. The agreement is reasonable and quite consistent in momentum dependence with independent studies done by others in the collaboration, although not in absolute value because of differing selection criteria. The larger data/Monte Carlo discrepancies at low momenta are not unexpected, as the simulation of soft tracks and kaon decays-in-flight is suspect. (The apparent discrepancy at high momentum is probably a statistical fluctuation.) This tool is now finished and will be used to finalize the systematic uncertainties in the non-$D\bar{D}$ measurement over the next few months.

The BESIII collaboration currently has two "competing" sets of tools for tagging D mesons by full reconstruction in open-charm production and decay measurements. Cronin-Hennessy is the chair of the committee charged with cross-checking and evaluating these tools and the first comparison

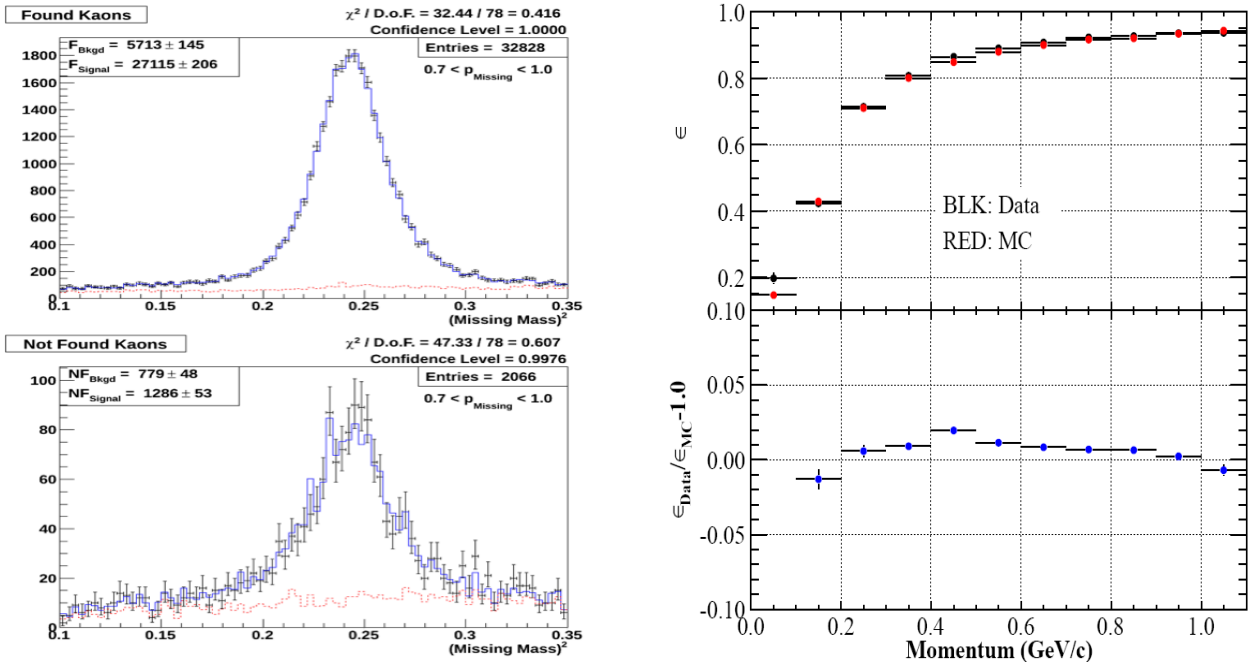

Figure 26: Left: example missing-mass-squared distributions for BESIII $\psi(3770)$ data tracking-efficiency study for kaon-found (top) and kaon-not-found (bottom) subsamples. Right: data/Monte Carlo tracking-efficiency comparison from fits for all momentum ranges.

studies have been done by Andy Julin. The two algorithms are dubbed DTagAlg and SD0TagAlg. They have been completely independently developed and have extensive menus of decay modes selected by the usual variables of beam-constrained mass and consistency with energy conservation. The two algorithms have so far been compared in a study of 15 D^0 tag modes using samples of events generated on the Minnesota farm under the standard version of BOSS for open-charm analyses (6.6.2). It is observed that DTagAlg (adapted to BESIII from CLEO code by CMU and Minnesota) has a speed advantage over SD0TagAlg, but that SD0TagAlg shows higher efficiency with only slightly higher background in some modes. This performance advantage is likely due to differences in particle identification and in the use by SD0TagAlg of constrained-vertex fitting. The latter would also explain the difference in CPU usage. These effects are being studied now and a similar study of charged-D tagging will follow. The final outcome of this work will be a standardized set of procedures implemented in both algorithms.

4.5 BESIII Analysis Projects in Progress

Minnesota group personnel are currently engaged in three analysis projects. The most ambitious is the effort to measure the branching fraction $\mathcal{B}(\psi(3770) \to \text{non}-D\bar{D})$. This has previously been measured by BESII and CLEO-c, and there is a discrepancy between the two measurements. With 2.9/fb of $\psi(3770)$ data, more than triple CLEO-c's sample, our goal in BESIII is to make a definitive determination of whether the non-$D\bar{D}$ rate is $\sim 15\%$ as claimed by BESII [52] or not significantly greater than zero, as found by CLEO-c [53, 54]. The underlying interest in this measurement arises from our expectation that decays of $\psi(3770)$, the first resonance encountered above the threshold for producing pairs of open-charm mesons, should be dominated by the $D^0\bar{D}^0$ and D^+D^- final states. If non-open-charm final states occur at a rate larger than would be expected based on decays of the

narrow below-threshold resonances, then this would be an indication that $\psi(3770)$ is not the simple quarkonium state previously assumed. Anything over a few percent non-$D\bar{D}$ decays is a definite surprise. It is worth noting that so far no exclusive non-$D\bar{D}$ final states have been observed that support the large BESII value.

To measure non-$D\bar{D}$ production we make two separate but coordinated measurements using BESIII data. Derrick Toth focuses on using D-tagging tools to measure the yields of single- and double-tag $D\bar{D}$ events from which $N_{D\bar{D}}$ can be extracted. Jianming Bian has designed hadronic-event-selection cuts and background-estimation to measure $N_{\psi(3770)}$. The latter determination is more straightforward in principle, but more problematic in execution.

The background-subtracted yield of hadronic events in $\psi(3770)$ decays is given by

$$N_{\psi(3770)} = N_{\text{on-}\psi(3770)} - N_{q\bar{q}} - N_{\psi(2S)} - N_{J/\psi} - \Sigma_{l=\tau,\mu,e} N_{\ell^+\ell^-} - N_{two-photon},$$

where $N_{\text{on-}\psi(3770)}$ is the observed number of hadronic events at the $\psi(3770)$ peak; $N_{q\bar{q}}$ is the number of observed hadronic events from continuum $q\bar{q}$ production ($q = uds$); $N_{\psi(2S)}$ and $N_{J/\psi}$ are the number of hadronic events from decays of $\psi(2S)$ and J/ψ decays produced primarily by initial-state radiation down to the narrow $c\bar{c}$ resonances; $N_{\ell^+\ell^-}$ is the number of events from $e^+e^- \to \ell^+\ell^-$; and $N_{two-photon}$ is the number of hadron events from two-photon fusion. Among these, $q\bar{q}$ is the largest and most difficult to determine with the required precision. Our default procedure is to determine $N_{q\bar{q}}$ by scaling the number of hadrons observed in continuum data at $\text{E}_{\text{CM}} = 3650$ MeV, where BESIII collected an integrated luminosity of 45 pb^{-1}:

$$N_{q\bar{q}} = N_{q\bar{q}}(3650) \cdot S, \text{and}$$

$$S = \frac{\mathcal{L}(3773)}{\mathcal{L}(3650)} \frac{eff(3773)}{eff(3650)} \left(\frac{3.650}{3.773}\right)^2.$$

In this equation S is the scale factor between $\text{E}_{\text{CM}} = 3650$ MeV and $\text{E}_{\text{CM}} = 3773$ MeV; $\mathcal{L}(3773)$ and $\mathcal{L}(3650)$ are the integrated luminosities; and $eff(3650)$ and $eff(3773)$ are the event-selection efficiencies. Because the corrections are large and the non-$D\bar{D}$ rate is small, our measurement is very dependent on the reliable determination of S.

The efficiency ratio $\frac{eff(3773)}{eff(3650)}$ has been studied with Monte Carlo. Surprisingly, the two independent $q\bar{q}$ Monte Carlo generators used by BESIII give efficiency ratios differing by $\sim 4\%$. Furthermore, they fail to reproduce critical features of continuum hadronic events in data, such as the charged-track multiplicity distribution. Because the cross section for $q\bar{q}$ is roughly double that for $D\bar{D}$, this leads to a dominant and unacceptable systematic uncertainty in $\mathcal{B}(\text{non}-D\bar{D})$. For this reason, to complete the measurement we have requested additional BESIII data to reliably determine $\frac{eff(3773)}{eff(3650)}$. Specificallly we will collect data at five points ($\text{E}_{\text{CM}} = 3500$ MeV, 3542 MeV, 3600 MeV, 3650 MeV, and 3671 MeV (~ 5 pb^{-1} for each), which, in combination with the previous data at 3650 MeV, will result in a systematic uncertainty associated with the efficiency ratio of about 1%. Fig. 28 shows the envelope of uncertainty that is expected for the extrapolation of the $q\bar{q}$ yield for correction at $\psi(3770)$. The new data will be collected in May 2013, allowing us to obtain final yields in the summer and to finalize this measurement by the end of 2013.

The measurement of the $D\bar{D}$ yield is obtained by measuring single- and double-tag event yields using standard D-tagging tools. If the number of single-tags in a particular decay mode i is N_i, the number in decay mode j is N_j, and the number of double tags (one in mode i and one in mode j) is N_{ij}, then the number of $D\bar{D}$ events can be expressed

$$N_{D\bar{D}} = \frac{N_i N_j \epsilon_{ij}}{N_{ij} \epsilon_i \epsilon_j},$$

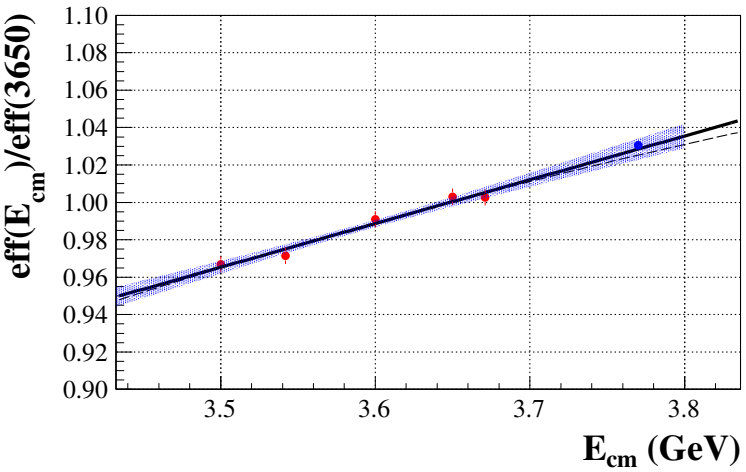

Figure 27: Performance of the selection-efficiency extrapolation in MC with 5 energy points, with linear and quadratic fits.

where ϵ_i and ϵ_j are the respective single-tag efficiencies and ϵ_{ij} is the double-tag efficiency determined by Monte Carlo simulation. Because this measurement is made with multiple tag modes, the final result for $N_{D\bar{D}}$ is determined as a weighted average over all combinations.

D tags are selected based on energy and momentum conservation expressed through the variables $\Delta E = E_{tag} - E_{beam}$ (~ 0 for signal) and $M_{BC} = \sqrt{E^2_{beam} - (\vec{p_{tag}})^2}$ (beam-constrained mass, peaks at the D mass). The analysis uses three D^0 decay modes ($K^-\pi^+$, $K^-\pi^+\pi^0$, $K^-\pi^+\pi^+\pi^-$) and six D^+ modes ($K^-\pi^+\pi^+$, $K^-\pi^+\pi^+\pi^0$, $K^0_S\pi^+$, $K^0_S\pi^+\pi^0$, $K^0_S\pi^+\pi^+\pi^-$, $K^+K^-\pi^+$), so there are 45 double-tag combinations. Special cuts suppress cosmic ray and QED backgrounds for modes with only two charged tracks. D-tag candidates are subjected to mode-specific ΔE cuts and M_{BC} distributions are constructed for fits to Monte Carlo-generated signal and background distributions (with smearing to account for imperfect detector modeling). The single-tag yields are then determined by a "cut-and-count" procedure within the M_{BC} signal region and combinatoric background is determined by integrating the fit-determined background function over the same range. A small additional correction is made for peaking backgrounds from other D modes. This technique is mature and has been extensively validated with Monte Carlo "in/out" testing.

A new procedure to determine the double-tag yields that more closely parallels the handling of single-tags has recently been developed. After a cut on ΔE, distributions of M_{BC1} vs. M_{BC2} (beam-constrained masses of the two Ds in the double-tag) are constructed and fitted in 2D to a combination of Monte Carlo (signal) and analytical (background) functions. This procedure has also been extensively tested with Monte Carlo and works very well. Fig. 27 shows an example fit for the $K^-\pi^+$ vs. $K^-\pi^+\pi^+\pi^-$ double-tag combination.

An advantage of the single-tag/double-tag technique is the expected cancellation of many systematic uncertainties, but extensive systematic studies are still needed. Toth has investigated sensitivity to the signal and background fit shapes in single- and double-tag fits, the best-candidate selection, data/Monte Carlo differences in ΔE resolution, and the selection criteria that suppress cosmic ray and QED contamination. Studies of the effects of potential mismodeling of resonant substructure,

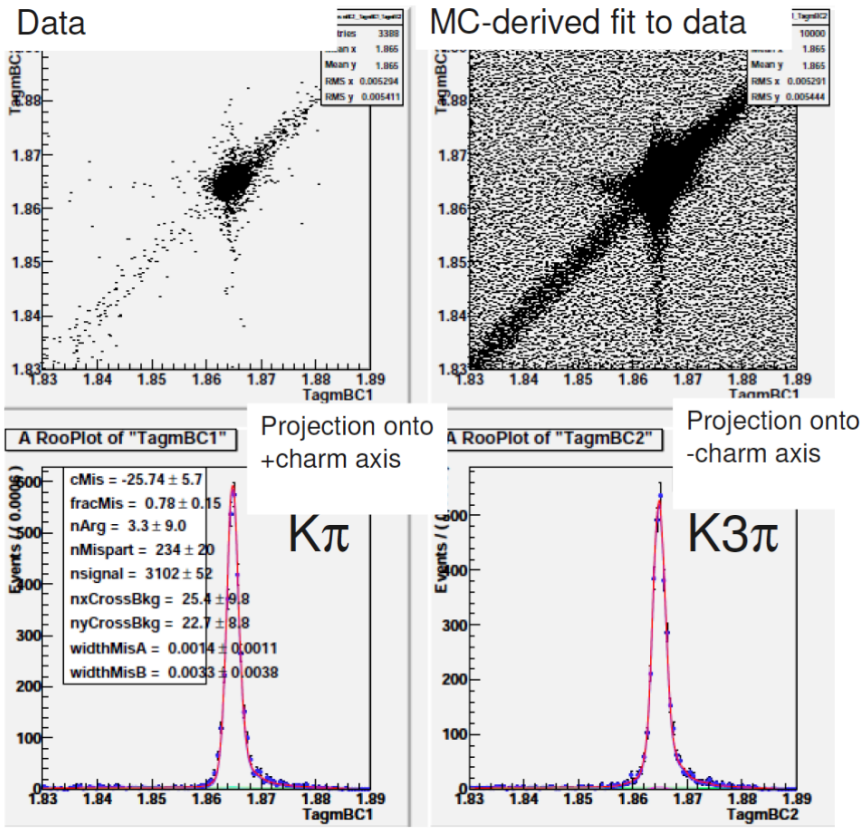

Figure 28: Example 2D fit to determine the $K^-\pi^+$ vs. $K^-\pi^+\pi^+\pi^-$ double-tag yield.

of the "other-side" event environment, of initial-state radiation, and of imperfect modeling of the tracking response of BESIII are ongoing.

Both the $D\bar{D}$ counting and the measurement of the hadronic-event yield have been developed and refined using Monte Carlo and the first one third of the 2.9/fb BESIII $\psi(3770)$ data sample. Once the systematic studies are complete and the new continuum data are in hand, we will unblind ourselves to the remaining data and extract final results.

The second area of Minnesota group analysis activity is a role in the search for and study of new charmonium-like states in BESIII data collected at 4260 MeV (1/fb analyzed so far, additional 2/fb expected), 4360 MeV (0.5/fb) and nearby energies (0.5/fb). BESIII recently submitted "Observation of a charged charmoniumlike structure in $e^+e^- \to pi^+pi^-J/\psi$ at $\sqrt{s} = 4.26$ GeV" to PRL [51]. This paper reports a measurement of the cross section for this final state that is consistent with BaBar, Belle and CLEO-c measurements, but also finds a structure of mass $3899.0 \pm 3.6 \pm 4.9$ MeV/c^2 and width $46 \pm 10 \pm 20$ MeV in the $\pi^\pm J/\psi$ mass spectrum. Because this state decays to charmonium and has nonzero electric charge, it must have a more complicated structure than $c\bar{c}$, such as a charm-meson molecule, tetraquark state or hybrid charmonium [55]. Detailed measurements of the properties of this Z_c state and searches for related objects, including neutrals, will be essential to elucidate its nature. Bian and Poling are now part of the "XYZ" group working on this in BESIII. Bian has analyzed all available data for the final state $\pi^0\pi^0 J/\psi$ and has made a preliminary observation of an enhancement near 3900 MeV, perhaps the neutral partner of the $Z_c^\pm$. This is not yet approved for presentation outside the collaboration, but Bian and Poling are working to

complete the analysis and submit a paper by summer 2013. A separate component of our XYZ effort will involve Bian, Julin and Poling working on a comprehensive set of measurements of the cross sections for two-body and multi-body final states including charm meson-antimeson pairs and 0, 1 or (perhaps) 2 pions. This is an extension of techniques developed by Brian Lang (former Minnesota student) and Poling on CLEO-c data [56].

Our third current analysis project is that of undergraduate student Nick Smith, who is working under the supervision of Cronin-Hennessy on a measurement of the $\psi(3770)$ resonant line shape. He uses standard D-tagging tools to extract counts at each of 15 binned beam-energy ranges in BESIII scan data collected near 3770 MeV. Two dimensional distributions are constructed for selected D tags in the M_{BC} vs. ΔE plane and fitted to expected distributions for four physics components ($q\bar{q}$, $\tau\bar{\tau}$, radiative return to J/ψ and radiative return to ψ') determined from 100-times-data Monte Carlo samples. Nick has demonstrated that his procedure accurately recovers the input D cross section in Monte Carlo for the nine cleanest $D^{\pm}$ and D^0 modes. The complex fit to data has proved very challenging. Work is in progress to understand differences between the data and Monte Carlo, especially in the signal shape. Once Nick has demonstrated successful fits to the data, the cross sections for the 15 beam-energy bins can be extracted and then fitted to candidate line shapes (convoluted with an initial-state-radiation correction). This has been demonstrated by a successful in/out test in Monte Carlo. The next steps will be adding decay modes for data, and correcting issues found in the Monte Carlo in-out test. The active analysis phase of this project should be completed by the time that Nick leaves Minnesota at the end of summer 2013.

4.6 Completed Papers and Other Analysis Activities

In 2012 we published two BESIII papers with major authorship from Minnesota. The first was "Study of $\psi(3686) \to \pi^0 h_c$, $h_c \to \gamma\eta_c$ via η_c exclusive modes" [57]. Bian was one of two principal authors. This was an extension of his work that was reported in the first PRL produced by BESIII in 2010 ("Measurements of $h_c(^1P_1)$ in ψ' Decays," [58]), a paper for which Poling was on the analysis committee. The new and more detailed study used the same data sample to measure the mass and width of the P-wave charmonium spin-singlet state $h_c(^1P_1)$. The technique was simultaneous fitting of the distributions of the π^0 recoil mass for 16 exclusive η_c decay modes. The results included mass and width measurements ($M_{(hc)} = 3525.31 \pm 0.11(\text{stat.}) \pm 0.14(\text{syst.})$ MeV/c^2 and $\Gamma(h_c) = 0.70 \pm 0.28 \pm 0.22$ MeV) consistent with and more precise than previous measurements, and new measurements of the 16 exclusive η_c branching fractions, five of them first measurements. It also included new measurements of the η_c line-shape parameters in $h_c \to \gamma\eta_c$ ($M(\eta_c) = 2984.49 \pm 1.16 \pm 0.52$ MeV/c^2 and $\Gamma(\eta_c) = 36.4 \pm 3.2 \pm 1.7$ MeV) made by simultaneously fitting hadronic mass spectra for the 16 η_c decay channels. Poling provided some of the oversight for the completion of the analysis and was heavily involved in writing the paper.

The second paper in 2012 was "Study of $J/\psi \to p\bar{p}$ and $J/\psi \to n\bar{n}$, for which Bian was the primary author and Poling provided oversight and help in drafting and finalizing the manuscript. This analysis was based on 225.2 million J/ψ decays and was the first BESIII analysis involving detection of antineutrons. Because the process is an octet-baryon-pair decay, it is seen as a good test of PQCD (the three gluons in the OZI-violating strong decay match the three $q\bar{q}$ pairs). The ratio between the branching frations provides information about the phase between the strong and EM amplitudes in the process. The branching fractions are determined to be $\mathcal{B}(J/\psi \to p\bar{p})) = (2.112 \pm 0.004 \pm 0.031) \times 10^3$ and $\mathcal{B}(J/\psi \to n\bar{n} = (2.07 \pm 0.01 \pm 0.17) \times 10^3$. Distributions of the angle between the proton or anti-neutron and the beam direction were measured and found to be

well described by $1+\alpha\cos^2\theta$, giving $\alpha = 0.595 \pm 0.012 \pm 0.015$ and $\alpha = 0.50 \pm 0.04 \pm 0.21$ for $p\bar{p}$ and $n\bar{n}$, respectively, suggesting a large phase angle between the strong and electromagnetic amplitudes in $J/\psi \to N\bar{N}$.

Bian also played an important role in "Two-photon widths of the $\chi_{c0,2}$ states and helicity analysis for $\chi_{c2} \to \gamma\gamma$ [59]. This analysis was led by Tao Luo (Hawaii), and Bian worked on developing event-selection code, helping with background analysis, fitting the helicity amplitude, cross-checking the results, and drafting the paper.

The Minnesota group also had significant involvement in a number of other completed and ongoing BESIII analysis projects as members of analysis committees. Poling worked on the PRL "First observation of the $M1$ transition $\psi \to \gamma\eta_c(2S)$," [60], providing input based on experience from the previous CLEO-c search [61] (Minnesota thesis of Kaiyan Gao) and helping finalize the selection, specifying systematic studies and drafting the paper. The technique was similar to CLEO-c, but the larger data sample and a clever technique for constructing and fitting the mass distribution led to success where CLEO-c had failed. Poling also was the chair of the committees reviewing BESIII D^0 and D^+ semileptonic decay measurements during the preparation of initial preliminary results in 2012. He has recently passed that responsibility on to our new research associate Muramatsu. Poling is also on the analysis committee for "Dalitz Analysis of the Decay $D^\pm \to K_S\pi\pi$." Cronin-Hennessy's BESIII committees have been the D-tag evaluation/comparison mentioned previously, the completed "Higher-order multipole amplitude measurement in $\psi(2S) \to \gamma\chi_{c2}$ [62]" and "Search for CP/P-violation process pseudoscalar decays into $\pi\pi$ [63]. Bian has also served on several paper committees, including the multipole amplitude measurement with Cronin-Hennessy. His current assignments are "Measurement of $\psi(3770) \to \gamma\chi_{cJ}$, "Measurements of the luminosity at 3.773 GeV and 3.650 GeV," "The study of $J/\psi \to p\bar{p}a_0(980)$," and "Analysis of $\psi(3770) \to p\bar{p}$ and $p\bar{p}\pi^0$."

Appendix 1: Bibliography and References

References

[1] S. Chatrchyan *et al.* [CMS Collaboration], "Observation of a new boson at a mass of 125 GeV with the CMS experiment at the LHC," Phys. Lett. B **716**, 30 (2012) [arXiv:1207.7235 [hep-ex]].
S. Chatrchyan *et al.* [CMS Collaboration], "A New Boson with a Mass of 125 GeV Observed with the CMS Experiment at the Large Hadron Collider," Science **338**, 1569 (2012).

S. Chatrchyan *et al.* [CMS Collaboration], "Observation of a new boson with mass near 125 GeV in pp collisions at sqrt(s) = 7 and 8 TeV," JHEP **06**, 081 (2013) [arXiv:1303.4571 [hep-ex]].

[2] CMS Collaboration [J. Mans, editor], *CMS Technical Design Report for the Phase 1 Upgrade of the Hadron Calorimeter*, CERN-LHCC-2012-015.

[3] V. Khachatryan *et al.* [CMS Collaboration], "Measurement of the Isolated Prompt Photon Production Cross Section in *pp* Collisions at $\sqrt{s}$ = 7 TeV," Phys. Rev. Lett. **106** (2011) 082001 [arXiv:1012.0799 [hep-ex]].

S. Chatrchyan *et al.* [CMS Collaboration], "Measurement of the Differential Cross Section for Isolated Prompt Photon Production in pp Collisions at 7 TeV," Phys. Rev. D **84**, 052011 (2011) [arXiv:1108.2044 [hep-ex]].

[4] 'Energy calibration and resolution of the CMS electromagnetic calorimeter in pp collisions at $\sqrt(s)$ = 7 TeV,' The CMS Collaboration, arXiv:1306.2016v1 [hep-ex] Submitted to JINST.

[5] S. Chatrchyan *et al.* [CMS Collaboration], "Measurement of the Rapidity and Transverse Momentum Distributions of Z Bosons in pp Collisions at sqrt(s)=7 TeV," Phys. Rev. D. **85**, 032002 (2012) [arXiv:1110.4973 [hep-ex]].

[6] A. Banfi, S. Redford, M. Vesterinen, P. Waller and T. R. Wyatt, "Optimisation of variables for studying dilepton transverse momentum distributions at hadron colliders," Eur. Phys. J. C **71**, 1600 (2011) [arXiv:1009.1580 [hep-ex]].

[7] G.F. Giudice and R. Rattazzi, "Theories with gauge-mediated supersymmetry breaking," Phys. Rept. **322**, 419 (1999), doi:10.1016/S0370-1573(99)00042-3, [arXiv:9801271 [hep-ph]].

[8] S. Chatrchyan *et al.* [CMS Collaboration], "Search for long-lived particles in events with photons and missing energy in proton-proton collisions at $\sqrt{s}$ = 7 TeV ," Phys. Lett. **722**, 273 (2013) [arXiv:1212.1838 [hep-ex]].

[9] S. Chatrchyan *et al.* [CMS Collaboration], "Search for new physics in events with photons, jets, and missing transverse energy in pp collisions at $\sqrt{s}$ = 7 TeV ," JHEP **03**, 111 (2013) [arXiv:1212.4784 [hep-ex]].

[10] S. Chatrchyan *et al.* [CMS Collaboration], "Search for heavy long-lived charged particles in pp collisions at $\sqrt{s}$ = 7TeV ," Phys. Lett. **713**, 408 (2012) [arXiv:1205.0272 [hep-ex]];

[11] S. Chatrchyan *et al.* [CMS Collaboration], "Searches for long-lived charged particles in pp collisions at $\sqrt{s} = 7$ and 8 TeV," JHEP **07**, 122 (2013) [arXiv:1305.0491 [hep-ex]].

[12] S. Chatrchyan *et al.* [CMS Collaboration], "Searches for long-lived charged particles in pp collisions at $\sqrt{s}$=7 and 8 TeV," arXiv:1305.0491 [hep-ex].

[13] S. Chatrchyan *et al.* [CMS Collaboration], "Search for heavy neutrinos and W[R] bosons with right-handed couplings in a left-right symmetric model in pp collisions at sqrt(s) = 7 TeV," Phys. Rev. Lett. **109**, 261802 (2012) [arXiv:1210.2402 [hep-ex]].

[14] A. Barysevich, *et al.*, "Radiation damage of heavy crystalline detector materials by 24-GeV protons," Nucl. Instrum. Meth. A **701**, 231 (2013).

[15] "Test beam evaluation of CMS ECAL EE Super Crystal made of gamma- and hadron-damaged crystals," M. Ambrose E_{T}al. CMS DN -2013/007.

[16] "Feasibility study of a Fused Quartz detector for measuring the Machine Induced Background in the CMS Cavern," M. J. Ambrose, A. E. Dabrowski, M. Giunta, S. Orfanelli, R. Rusack, D. Stickland. CMS DN -2013/004.

[17] "Gas Electron Multiplier (GEM) Detectors, Principles of Operation and Applications," F. Sauli, RD51-NOTE-2012-007 REVISED 21.09.2012.

[18] "A spark-resistant bulk-micromegas chamber for high-rate applications", T. Alexopoulos et al. NIM A 640 (2011) 110-118

[19] "DELPHES 3, A modular framework for fast simulation of a generic collider experiment." J. de Favereau, *et al.*, arXiv:1307.6346 [hep-ex].

[20] "Particle flow calorimetry and the Pandora PFA algorithm," M. Thomson, NIM A611(2009) 2540, and "Performance of particle flow calorimetry at CLIC," J.S. Marshall, A.Munnich and M.A.Thomson, NIM A700(2013)153162.

[21] Z. Ahmed et al. (CDMS Collaboration), *Dark Matter Search Results from the CDMS II Experiment*, Science **327**, 1619 (2010) [arXiv:0912.3592].

[22] Z. Ahmed et al. (CDMS Collaboration), *Results from a Low-Energy Analysis of the CDMS II Germanium Data*, Phys. Rev. Lett. **106**, 131302 (2011).

[23] D.S. Akerib et al. (CDMS Collaboration), *Low-threshold analysis of CDMS shallow-site data*, Phys. Rev. D **82**, 122004 (2010).

[24] Z. Ahmed et al. (CDMS Collaboration), *Analysis of the low-energy electron-recoil spectrum of the CDMS experiment*, Phys. Rev. D **81**, 042002, (2010) [arXiv:0907.1438].

[25] R. Agnese et al. (CDMS Collaboration), *Dark Matter Search Results Using the Silicon Detectors of CDMS II*, submitted to Phys.Rev.Lett. May 1, 2013 [arXiv:1304.4279].

[26] R. Agnese et al. (CDMS Collaboration), *Silicon Detector Results from the First Five-Tower Run of CDMS II*, Phys. Rev. D 88, 031104(R) (2013) [arXiv:1304.3706].

[27] Z. Ahmed et al. (CDMS Collaboration), *Search for annual modulation in low-energy CDMS-II data*, [arxiv:1203.1309].

[28] Z. Ahmed et al. (CDMS Collaboration), *Search for inelastic dark matter with the CDMS II experiment*, Phys. Rev. D **83**, 112002 (2011), [arXiv:1012.5078].

[29] Z. Ahmed et al. (CDMS Collaboration), *Search for Axions with the CDMS Experiment*, Phys. Rev. Lett **103**, 141802 (2009) [arXiv:0902.4693].

[30] Z. Ahmed et al. (CDMS Collaboration and Edelweiss Collaboration), *Combined limits on WIMPs from the CDMS and EDELWEISS experiments*, Phys. Rev. D **84**, 011102 (2011).

[31] R. Agnese et al. (CDMS Collaboration), *Demonstration of Surface Electron Rejection with Interleaved Germanium Detectors for Dark Matter Search*, submitted to Phys. Rev. Lett., May 10 2013, [arXiv:1305.2405].

[32] J. Billard, L. Strigari, and E. Figueroa-Feliciano, Implication of neutrino backgrounds on the reach of next generation dark matter direct detection experiments, [arXiv:1307.5458].

[33] E. Armengaud et al. (EDELWEISS-II Collaboration), *Final results of the EDELWEISS-II WIMP search using a 4-kg array of cryogenic germanium detectors with interleaved electrodes*, Phys. Lett. B **702**, 329 (2011), [arXiv:1103.4070].

[34] E. Aprile et al. (XENON10 Collaboration), *Dark Matter Results from 100 Live Days of XENON100 Data*, Phys. Rev. Lett. **107**, 131302 (2011), [arXiv:1104.2549v2].

[35] G. Angloher et al. (CRESST-II Collaboration), *Results from 730 kg days of the CRESST-II Dark Matter Search*, [arXiv:1109.0702].

[36] D. Hooper, J.I Collar, J. Hall, D. McKinsey, and C.M. Kelso, *Consistent dark matter interpretation for CoGeNT and DAMA/LIBRA*, Phys. Rev. D. **82**, 123509 (2010).

[37] R. Bernabei et al. (DAMA/LIBRA Collaboration), *New results from DAMA/LIBRA*, European Physical Journal C **67**, 39 (2010), [arXiv:1002.1028].

[38] C.E. Aalseth et al. (CoGeNT Collaboration), *Results from a Search for Light-Mass Dark Matter with a p-Type Point Contact Germanium Detector*, Phys. Rev. Lett. **106**, 131301 (2011).

[39] C. Strege, G. Bertone, D. G. Cerdeno, M. Fornasa, R. Ruiz de Austri, R. Trotta, *Updated global fits of the cMSSM including the latest LHC SUSY and Higgs searches and XENON100 data*, J. Cosmol. Astropart. Phys. **03**, 030, (2012), [arXiv:1112.4192].

[40] D.A. Bauer, S. Burke, J. Cooley, M. Crisler, P. Cushman, F. DeJongh, L. Duong, R. Ferril, S.R. Golwala, J. Hall, D. Holmgren, R. Mahapatra, H. Nelson, A. Reisetter, J. Sander, and C. Savage, *The CDMS II Data Acquisition System*, Nucl. Inst. and Meth. A **638**, 127 (2011).

[41] E. Armengaud et al. (EDELWEISS Collaboration), *Search for low-mass WIMPs with EDELWEISS-II heat-and-ionization detectors*, Phys. Rev. D **86**, 051701 (2012), [arXiv:1207.1815].

[42] J. Angle et al. (XENON Collaboration), *Search for Light Dark Matter in XENON10 Data*, Phys. Rev. Lett. **107**, 051301 (2011), [arXiv:1104.3088].

[43] J. Angle et al. (XENON Collaboration), *First Results from the XENON10 Dark Matter Experiment at the Gran Sasso National Laboratory*, Phys. Rev. Lett. **100**, 021303 (2008).

[44] C. Kelso, D. Hooper, and M. R. Buckley, *Toward a consistent picture for CRESST, CoGeNT, and DAMA*, Phys. Rev. D **85**, 043515 (2012), [arXiv:1110.5338].

[45] J. Lindhard et al., Mat. Fys. Medd. Dan. Vid. Selsk. **33**, no 10 (1963).

[46] A.L Fitzpatrick, W. Haxton, E. Katz, N. Lubbers, and Y. Xu, *The Effective Field Theory of Dark Matter Direct Detection*, [arXiv:1203.3542].

[47] A.L Fitzpatrick, W. Haxton, E. Katz, N. Lubbers, and Y. Xu, *Model Independent Direct Detection Analyses*, [arXiv:1211.2818].

[48] H. Chagani et al. (SuperCDMS Collaboration), *Ionization Measurements of SuperCDMS SNOLAB 100 mm Diameter Germanium Crystals*, J. Low Temp. Phys. **167**, 1125 (2012).

[49] L. Ovechkina et al. *Gadolinium loaded plastic scintillators for high efficiency neutron detection*, Phys. Proc. **2** 161 (2009) [http://dx.doi.org/10.1016/j.phpro.2009.07.008].

[50] B.P. Abbott et al. (The LIGO Scientific Collaboration and The Virgo Collaboration), *An Upper Limit on the Stochastic Gravitational-wave Background of Cosmological origin*, Nature **460**, 990 (2009).

[51] M. Ablikim *et al.* [BESIII Collaboration], arXiv:1303.5949 [hep-ex].

[52] M. Ablikim *et al.* [BES Collaboration], Phys. Lett. B **659**, 74 (2008).

[53] D. Besson *et al.* [CLEO Collaboration], Phys. Rev. Lett. **96**, 092002 (2006) [Erratum-ibid. **104**, 159901 (2010)] [hep-ex/0512038].

[54] D. Besson *et al.* [CLEO Collaboration], Phys. Rev. Lett. **104**, 159901 (2010) [arXiv:1004.1358 [hep-ex]].

[55] M. B. Voloshin, arXiv:1304.0380 [hep-ph].

[56] D. Cronin-Hennessy *et al.* [CLEO Collaboration], Phys. Rev. D **80**, 072001 (2009) [arXiv:0801.3418 [hep-ex]].

[57] M. Ablikim *et al.* [BESIII Collaboration], Phys. Rev. D **86**, 092009 (2012) [arXiv:1209.4963 [hep-ex]].

[58] M. Ablikim *et al.* [BESIII Collaboration], Phys. Rev. Lett. **104**, 132002 (2010) [arXiv:1002.0501 [hep-ex]].

[59] M. Ablikim *et al.* [BESIII Collaboration], Phys. Rev. D **85**, 112008 (2012) [arXiv:1205.4284 [hep-ex]].

[60] M. Ablikim *et al.* [BES Collaboration], Phys. Rev. Lett. **109**, 042003 (2012) [arXiv:1205.5103 [hep-ex]].

[61] D. Cronin-Hennessy *et al.* [CLEO Collaboration], Phys. Rev. D **81**, 052002 (2010) [arXiv:0910.1324 [hep-ex]].

[62] M. Ablikim *et al.* [BESIII Collaboration], Phys. Rev. D **84**, 092006 (2011) [arXiv:1110.1742 [hep-ex]].

[63] M. Ablikim *et al.* [BESIII Collaboration], Phys. Rev. D **84**, 032006 (2011) [arXiv:1106.5118 [hep-ex]].